AD-A073 417 ELECTRONICS RESEARCH LAB ADELAIDE (AUSTRALIA) F/G 4/1
PRELIMINARY ASSESSMENT OF INFRA-RED TRANSMISSION DATA MEASURED --ETC(U)
MAR 79 D R CUTTEN

UNCLASSIFIED ERL-0063-TM NL

| OF |
AD
A073417

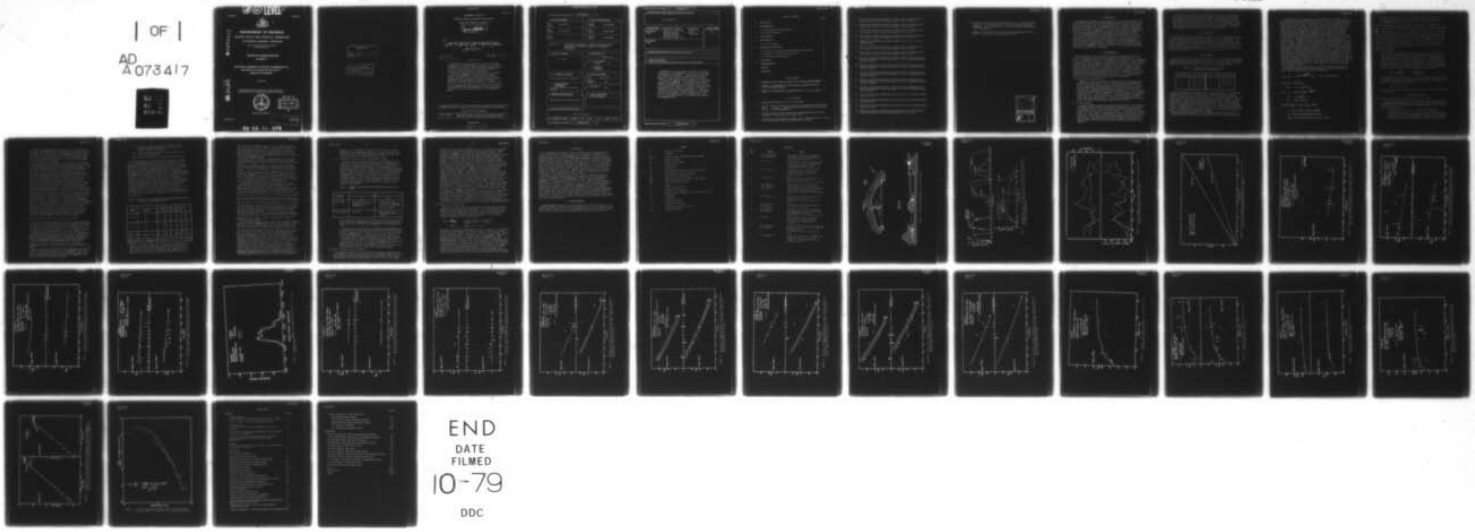

END
DATE
FILMED
10-79
DDC

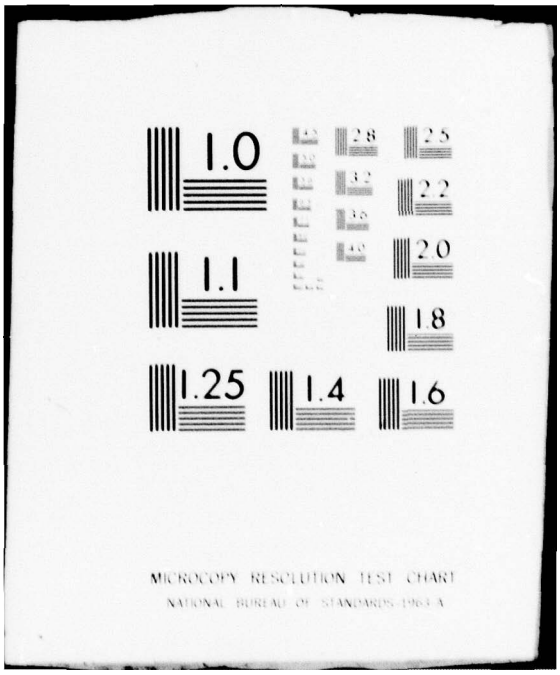
1.0
1.1
1.25
1.4
1.6
2.8
3.2
3.6
4.0
2.5
2.2
2.0
1.8
MICROCOPY RESOLUTION TEST CHART
NATIONAL BUREAU OF STANDARDS-1963-A

(12) LEVEL II

ERL-0063-TM

AR-001-623

AUSTRALIA

DEPARTMENT OF DEFENCE

DEFENCE SCIENCE AND TECHNOLOGY ORGANISATION

ELECTRONICS RESEARCH LABORATORY

DEFENCE RESEARCH CENTRE SALISBURY
SOUTH AUSTRALIA

AD A073417

TECHNICAL MEMORANDUM

ERL-0063-TM

PRELIMINARY ASSESSMENT OF INFRARED TRANSMISSION DATA MEASURED OVER 'OCEAN-TYPE' WATERS IN A TEMPERATE ENVIRONMENT

D.R. CUTTEN

DDC FILE COPY

Technical Memoranda are of a tentative nature, representing the views of the author(s), and do not necessarily carry the authority of the Laboratory.

DEFENCE SCIENCE AND TECHNOLOGY ORGANISATION

Approved for Public Release.

MARCH 1979

COPY No. 42

AR-001-623

DEPARTMENT OF DEFENCE

DEFENCE SCIENCE AND TECHNOLOGY ORGANISATION

ELECTRONICS RESEARCH LABORATORY

410 863

(9) TECHNICAL memoir

(14) ERL-0063-TM

(6) PRELIMINARY ASSESSMENT OF INFRA-RED TRANSMISSION DATA MEASURED OVER 'OCEAN-TYPE' WATERS IN A TEMPERATE ENVIRONMENT.

(10) D.R. Cutten

(12) 43 p.

(11) Mar 79

S U M M A R Y

Measurements have been made of the near sea infra-red transmission of the atmosphere over paths of 5 and 9 km in a temperate environment. Seven broadband spectral regions have been used and variations with absolute humidity, temperature and visibility are investigated.

The data are compared with the predictions of the AFGL computer model LOWTRAN3B. A discrepancy has appeared between the measured and calculated data for the 4.4 to 5.4 μm region due, possibly, to either no water continuum absorption being included in the model or an under-estimation of the N_2^C continuum absorption. Indications are that the dependence of water vapour continuum transmission on precipitable water and temperature in the 8.2 to 11.8 μm region may not be accurately described by the LOWTRAN3B model.

micrometers

POSTAL ADDRESS: Chief Superintendent, Electronics Research Laboratory, Box 2151, G.P.O., Adelaide, South Australia, 5001.

410 863

DOCUMENT CONTROL DATA SHEET

Security classification of this page: UNCLASSIFIED

1 DOCUMENT NUMBERS	
AR Number:	AR-001-623
Report Number:	ERL-0063-TM
Other Numbers:	

2 SECURITY CLASSIFICATION	
a. Complete Document:	UNCLASSIFIED
b. Title in Isolation:	UNCLASSIFIED
c. Summary in Isolation:	UNCLASSIFIED

3 TITLE: PRELIMINARY ASSESSMENT OF INFRARED TRANSMISSION DATA MEASURED OVER 'OCEAN-TYPE' WATERS IN A TEMPERATE ENVIRONMENT

4 PERSONAL AUTHOR(S):

D.R. Cutten

5 DOCUMENT DATE: March 1979

6 6.1 TOTAL NUMBER OF PAGES: 40

6.2 NUMBER OF REFERENCES: 11

7 7.1 CORPORATE AUTHOR(S):

Electronics Research Laboratory

7.2 DOCUMENT SERIES AND NUMBER

Electronics Research Laboratory 0063-TM

8 REFERENCE NUMBERS

a. Task: NAV 77/141

b. Sponsoring Agency: DST

9 COST CODE: 367022

10 IMPRINT (Publishing organisation)

Defence Research Centre Salisbury

11 COMPUTER PROGRAM(S) (Title(s) and language(s))

12 RELEASE LIMITATIONS (of the document):

For Public Release.

12.0	OVERSEAS	NO		P.R.	1	A		B		C		D		E	

Security classification of this page: UNCLASSIFIED

Security classification of this page: UNCLASSIFIED

13 ANNOUNCEMENT LIMITATIONS (of the information on these pages):

No limitation

14 DESCRIPTORS:

a. EJC Thesaurus Terms

Atmospheric physics
Atmospheric scattering
Infrared sources
Infrared radiation
Infrared spectra
Atmospheric refraction
Atmospheric composition
Earth atmosphere

b. Non-Thesaurus Terms

15 COSATI CODES

0401

16 LIBRARY LOCATION CODES (for libraries listed in the distribution):

17 SUMMARY OR ABSTRACT:
(if this is security classified, the announcement of this report will be similarly classified)

Measurements have been made of the near sea infrared transmission of the atmosphere over paths of 5 and 9 km in a temperate environment. Seven broad-band spectral regions have been used and variations with absolute humidity, temperature and visibility are investigated.

The data are compared with the predictions of the AFGL computer model LOWTRAN3B. A discrepancy has appeared between the measured and calculated data for the 4.4 to 5.4 μm region due, possibly, to either no water continuum absorption being included in the model or an underestimation of the N_2 continuum absorption. Indications are that the dependence of water vapour continuum transmission on precipitable water and temperature in the 8.2 to 11.8 μm region may not be accurately described by the LOWTRAN3B model.

Security classification of this page: UNCLASSIFIED

TABLE OF CONTENTS

LIST OF TABLES

LIST OF FIGURES

21. Comparison of Average Transmissions Measured Over a Given Pathlength in the 8.2 to 11.8 μm and 10.52 to 10.70 μm Spectral Regions with LOWTRAN3B. Data are Plotted for a Given Water Vapour Concentration at all Temperatures

22. Example of a Maritime Aerosol Size Distribution Measured at Victor Harbor on a Day where the Visual Range was 60 km

1. INTRODUCTION

A measurement programme has been initiated to collect infra-red (IR) atmospheric transmission data in various broadband spectral regions between 1 and 12 μm over long paths near the air-sea interface in a temperate environment. This work constitutes part of task NAVY 77/141 which involves a study of the parameters affecting the propagation of IR radiation through the atmosphere. The aim of the current programme is to obtain sufficient data on transmission in selected spectral regions for validating the predictions of the AFGL computer code LOWTRAN3B under similar meteorological conditions (ref. 1).

A preliminary assessment of transmission data measured over the period of November 1977 to April 1978 has been undertaken. It is the purpose of this short paper to report the effects of selected meteorological parameters (absolute humidity, temperature and visibility) on the IR atmospheric transmission in seven broadband spectral regions and compare these data with the predictions of LOWTRAN3B. Details of aerosol size distribution measurements made in this period are also included.

2. INSTRUMENTATION

The instrumentation used to measure absolute, broadband IR transmission through the atmosphere has already been described in detail (ref 2). In brief, the equipment consists of a van-mounted radiometer and a trailer-mounted, efficient, broadband IR source. The radiometer can measure the absolute transmission loss in selected spectral regions using a combination of three cooled detectors (PbS, InSb and MCT) and spectral filters. The IR source is a re-entrant, black-body cavity with an aperture of 100 cm^2, a nominal surface temperature of 975 K and total radiant power output of approximately 500 W. Both the IR source and radiometer are calibrated (as described in Ref. 2) to allow absolute transmission measurements to be made. The source radiation is chopped at 195 Hz for phase sensitive rectification of the received signal which gives good source discrimination against the background.

2.1 Meteorological instrumentation

During the actual transmission measurements five meteorological parameters were measured near the site. These parameters are temperature, relative humidity, visibility, mean wind speed and direction. The wet and dry temperatures were measured every ten minutes at the source end of the path with an Assmann psychrometer, and every five minutes at the radiometer end using ventilated platinum sensors (ref. 2). Two visibility meters were placed along the sightline to record the extinction coefficient continuously at $\lambda = 0.55$ μm (ref. 3). A Lambrecht-Woelfle anemometer located near the sightline provided data which when reduced, gave mean hourly wind speed and direction. Sea state was estimated using the scale given in the Bureau of Meteorology Observer's Guide (1973).

2.2 Aerosol sampling

Atmospheric particulate matter (aerosol) was sampled at the radiometer end of the sightline using 47 mm diameter Millipore filters with 0.05 μm ($\pm$ 0.003) pore size. The filter holder with suitable rain cover was mounted above the van about 3 m from the ground. A flowmeter was used to monitor the total volume of airpassing through the filter (about 4.6 ℓ/min) so that the total number of particles/unit volume/unit radius could be calculated. Total sampling time generally ranged from five to six hours. Filter samples were then stored in sealed containers until they were examined with a scanning electron microscope (SEM) as described in paragraph 4.1.

Preparation of samples for the SEM involved punching a 22 mm diameter disc out of the filter paper, mounting it on a suitable holder and coating to a thickness of 250 Å with carbon (150 Å) and gold/palladium (100 Å). The sample was then examined under a SEM at two magnifications where the scanned areas were selected randomly. The aim was to photograph at least 500 particles at each magnification for a particular sample. (Blank samples were prepared at different times to check that no contamination resulted from handling of the samples and the coating procedure.)

3. SITE SELECTION

Equipment used in making the transmission and meteorological measurements was located at Victor Harbor, a coastal site about 80 km south of Adelaide. This site was chosen as best suiting the requirements for open, 'ocean-type' sea conditions, prevailing on-shore winds not passing over continental land masses and low industrial contamination. Figure 1 shows the location of the two source sites, radiometer site and anemometer site. The topography at Port Elliot prevented the radiometer from being placed less than 20 m from the sea surface. Tidal height variation at the site is generally less than 1 m.

4. DATA ANALYSIS

During the period from November 1977 to April 1978, transmission measurements were made on 19 days for studying the variation in transmission with temperature, absolute humidity, visibility, wind and sea state. Data were measured for two pathlengths (5.03 and 9.05 km) in the spectral regions listed below.

TABLE 1: BROADBAND SPECTRAL REGIONS SELECTED FOR TRANSMISSION MEASUREMENTS

Filter No.	Region (μm)	Filter No.	Region (μm)
1	1.48 - 2.50	10	8.20 - 11.76
5	3.55 - 4.00	11	8.33 - 9.80
7	4.36 - 4.59	12	10.47 - 10.70
8	4.41 - 5.41		

Figure 2 reproduces the spectral curves of the filters used. The data were initially sorted to show the variability of transmission with a number of meteorological parameters. For the wind and sea state parameters, however, limited variation was experienced on the days measurements were made. Sea state varied between smooth and slight except for two days where moderate seas were experienced. Wind direction was predominantly SE to SW on 15 days with mean hourly wind velocities lying between 2.5 and 7 m/s. With such a restricted range in the wind and sea state parameters the data were not sorted for variability of transmission with these parameters. It is pointed out that the SE-SW wind is an on-shore wind and unlikely to contain any continental type aerosol because no large continental masses are nearby.

Barometric pressure recorded on the measurement days ranged from 1000 to 1027 millibars and consequently no assessment was based on pressure variations.

Visibility meters were located near the radiometer and at Granite Island to record visibilities above 30 km for each of the 19 days. The transmission data were grouped for scattering coefficients ($\sigma_{0.55\ \mu m}$) below or above 0.04 km^{-1} (visibility = $3.91/\sigma_{0.55\ \mu m}$). It should be noted that the temperature of the sample compartment of the visibility meter can be several degrees higher than ambient due to the small flow rate used. This could alter the localised relative humidity. Consequently, for high humidities the visibility meter reading may be higher than that prevailing. All readings for a relative humidity greater than 75% were distinguished from the rest of the data.

The temperature and absolute humidity were calculated from the wet and dry temperature data recorded at each end of the path. The mean trend of the data for each end was determined by eye and an average taken of the means at a particular time. Figure 3 reproduces such data from measurements made in one period. (The mean curve has not been drawn for clarity reasons.) On those days measurements were made the differences between the mean trend at each end of the path for absolute humidities between 6 and 12 gm/m^3 and for temperature, generally did not exceed 0.5 gm/m^3 and 1 °C respectively. On this basis, the uncertainty in absolute humidity along the whole path was assumed not to exceed this amount and accordingly the transmission data were plotted against precipitable water for 0.5 mm/km intervals. (Note that for a pathlength of 1 km, absolute humidity (ω) expressed in gm/m^3 equals precipitable water (ρ) expressed in mm/km.) Transmission data for each interval were averaged and the standard deviation calculated. In figures 5 to 16 which show the variation of transmission with precipitable water the points represent the average values and the bars the standard deviation limits. The number of measured data for each interval are also shown.

The magnitude of the transmission error arising from an uncertainty $\Delta\omega$ in the absolute humidity was calculated using the following expression for water vapour continuum transmission from LOWTRAN3B :

$$T_{H_2O\ cont} = \exp\left\{-\left(e^{6.08\left(\frac{296}{T}-1\right)}P_{H_2O} + \gamma\left(P_T - P_{H_2O}\right)\right)\omega RC_s^{\circ}(\nu)\right\} \qquad (1)$$

which can be rewritten as :

$$-\ln T = (K_1 - K_3)\omega^2 + K_2\omega$$

where $K_1 = \text{Const}\ C_s^{\circ}(\nu)RTe^{6.08\left(\frac{296}{T}-1\right)}$

$K_2 = 0.1\gamma\ P_T RC_s^{\circ}(\nu)$

$K_3 = \text{Const}\ C_s^{\circ}(\nu)\gamma\ RT$

therefore $\frac{dT}{T} = \{\ 2(K_1 - K_3)\omega + K_2\}\Delta\omega$

ω is the absolute humidity (gm/m^3)

P_T is the total atmospheric pressure

P_{H_2O} is the partial pressure for water vapour

$\gamma (= \frac{Cn}{Cs})$ the relative measure of the N_2-H_2O broadening absorption

$C_s^o(\nu)$ the self-broadening absorption coefficient for frequency ν and temperature 296K.

Figure 4 indicates the magnitude of $\frac{dT}{T}$ calculated at λ = 10.6μm where $\Delta\rho$ = 0.5 mm/km for the 2 pathlengths used. Similar curves were obtained when $\frac{dT}{T}$ is calculated for the 8.33 to 11.76μm region. The curve for the 9 km path indicates that the error can become significant for ρ over 10 mm/km and will increase when the temperature is below 296K because $\frac{dT}{T}$ is strongly dependant on temperature through the empirical expression $\exp(6.08(\frac{296}{T} - 1))$. However, the exact magnitude remains uncertain as γ = constant has been assumed. In the 3.55 to 4.00μm spectral regions $\frac{dT}{T}$ values are an order less when ρ approaches 20 mm/km.

4.1 Aerosol sizing

The size of the particles was determined from enlargements of photographs taken on the SEM by grouping the particles into specific size intervals. The intervals (48 in all) were based on the Zeiss particle counter which provides intervals of exponentially increasing width to improve the accuracy for the smaller particles. Circles define the 48 intervals etched onto a piece of transparent glass. The interval size to which a particle was allocated was chosen by treating the particle as a sphere with equivalent volume and selecting the circle with appropriate radius. The number of particles /cm^3/μm was determined from

$$n(r) = \frac{d\,N}{d(\log r)} = \frac{Ac}{aft\,\Delta\,(\log r)} \qquad (2)$$

where A denotes the total filter area in cm^2, a the counting area in cm^2, c the number of particles counted in one size interval (Δ (log r)), f the flow rate in cm^3/min and t the sampling time in minutes. The volume of particles in each interval is given by

$$V(r) = \frac{4}{3}\,\pi\,r^3\,n(r) \qquad (3)$$

which is useful for highlighting whether a particle distribution is single mode or bimodal.

5. RESULTS AND DISCUSSION

5.1 Variation of transmission with atmospheric parameters

In this section the variation of transmission with precipitable water and temperature are examined for five spectral regions. (Note that in figures 5 to 16 the bars represent the standard deviation levels for the data in each interval.)

5.1.1 Transmission variation in 3.5 to 4.0μm spectral region

Transmission data in this region exhibit a dependence on the water content in the path although not as strong as the variation which occurs in the 8 to 12μm region. Figures 5 and 6 reproduce the data for the two visibility groups considered. Even though

the data are scattered there does appear to be a trend towards an agreement with LOWTRAN3B over the 5 km range for both visibility intervals. For the 9 km range the LOWTRAN3B data appears to under-estimate the transmission when total precipitable water exceeds about 70 mm. (No suitable explanation can be offered at present as to why the transmission data for 9.2 mm/km precipitable water are similar for the two ranges.)

The limited data represented in figures 5 and 6 do not necessarily support the discrepancy which is now apparent between other measured and predicted transmission data recently reported for the 3.5 to 4.2 μm spectral region. These results will be briefly discussed. Laboratory measurements reporting values for the H_2O continuum absorption coefficient at 296K (White et al(ref.4)) indicate that the data of Burch et al(ref. 5), which is currently used in the LOWTRAN model, under-estimates the continuum absorption coefficient by as much as a factor of 2 near 3.6μm. The Burch data for 296K is most likely in error because of the extrapolation procedure used to obtain the room temperature data from measurements conducted at 338K: good agreement was obtained between the two groups of workers at this elevated temperature. In addition, the White data gives transmission values which compare more favourably than does Burch's data, with the H_2O continuum data deduced from high-resolution atmospheric transmission measurements conducted during high visibilities over water by the Naval Research Laboratory(ref. 6). Since such a significant discrepancy exists between the Burch and White data, the absorption coefficients measured by White et al have been incorporated into the LOWTRAN4 model to give a more representative 3.5 to 4.2μm continuum absorption. A revised exponential temperature dependence for C_S^O has also been derived from the absorption coefficients measured at the two temperatures. The value of γ in equ.(1) was still assumed to be 0.12. This brief review of data covering the 3.5 to 4.2μm region can only emphasise that as much data as possible must be collected to determine the precise dependence of atmospheric transmission data on absolute humidity and temperature.

5.1.2 Transmission variation in 4.4 to 5.4μm spectral region

The total transmission measured in the 4.4 to 5.4 μm region has been found to be lower than that predicted by LOWTRAN3B by as much as 20% for the 5 km range and 25% for 9 km range when visual range is greater than 30 km (see figures 7 and 8). Evidence of this discrepancy also appears in figures 17 to 22 of reference 1, where computed data are compared with Yates and Taylor data(ref. 7).

Further evidence on this discrepancy has also been deduced from measured high resolution transmission data recently published by Naval Research Laboratories(ref. 8). The average transmission in the 4.4 to 5.4μm region estimated using their data, (which had already been degraded with a triangular slit of half width 20 cm^{-1}) was found to be 32% lower than that calculated from LOWTRAN3B for a water vapour pressure of 11.3 mm Hg. over a 5.1 km path.

Since the measured aerosol extinction coefficient was small, the large discrepancy between the measured and LOWTRAN3B data in the present work cannot be explained by any inadequacy in the aerosol model. The under-estimation of transmission by LOWTRAN3B could arise from one or more of the following:

(i) the low resolution of the water and carbon dioxide absorption spectra arising from using the single parameter empirical band model,

(ii) no water vapour continuum absorption included in the model for this region, or

(iii) an under-estimation of the N_2 continuum absorption.

To examine if the low resolution spectral absorption calculations of LOWTRAN3B may account for this discrepancy, the high resolution model HITRAN model was used to calculate the average transmittance due to the spectral absorption of water and carbon dioxide. A wavenumber resolution of 0.05 cm^{-1} was selected for the high resolution calculations and results degraded with a triangular slit of half-width 20 cm^{-1} to make the data compatible with LOWTRAN3B. No aerosol extinction, water or nitrogen continuum absorption coefficients were included in the calculations. The exclusion of these coefficients can be done for comparison purposes because of the slowly varying nature of the coefficients with wavelength and hence, are essentially multiplicative factors.

Table 2 summarises the calculations made for several water vapour concentrations and ranges. (Calculations have been restricted because of the large computing times involved for this spectral region.) Up to the 10 km range the comparison is reasonable but as the range is increased further a large disagreement emerges where τ_{HI} is less than τ_{LO} by as much as 33% for a 30 km range.

TABLE 2: COMPARISON OF LOWTRAN3B AND HITRAN AVERAGE TRANSMISSIONS FOR 4.4 TO 5.4μm SPECTRAL REGION

Range (km)	Precipitable water (mm/km)	Average transmittance		$\frac{\tau_{LO}}{\tau_{HI}}$
		LOWTRAN3B	HITRAN	
5.03	7	.233	.242	.963
	10	.202	.208	.971
	13	.180	.184	.978
	17	.159	.161	.988
9.05	7	.165	.161	1.025
	10	.139	.136	1.022
	13	.122	.116	1.051
	17	.098	.105	1.069
20	13	.062	.051	1.216
30	13	.040	.030	1.333
Temperature: 21°C Pressure: 1013 mb Density of air: $1.191 \times 10^3 gm/m^3$				

However, it should be noted these calculations were made with an earlier version of the AFGL tape and two updated versions of the line compilation tape have been produced since April 1975 (the date of the tape used in this work). As line compilation errors are known to exist for the CO_2 and H_2O absorption lines on the

tape used, these comparisons will need to be repeated with the latest version of the tape. Figure 9 reproduces an example of the calculated spectra curves from the two models for this region. The calculated spectra do reveal some differences although it is noteworthy that the shape of the HITRAN curves for the 5.03 km path resembled more closely the measured curves given in reference 5 than did the LOWTRAN3B curves.

The results given in Table 2 appear, however, to be in direct conflict with similar calculations performed by Tuer(ref.9) who predicted that $T_{LO}/T_{HI} \leq 0.95$ for paths up to 40 km. Calculations undertaken in the present work for the same spectral interval (4.55 to 4.8μm) and meteorological conditions Tuer used, indicate $T_{LO}/T_{HI} > 1$ for similar pathlengths. As Tuer has included the nitrogen continuum absorption in his LOWTRAN calculations this would account for part of the discrepancy. However, the spectral shape of his HITRAN curves are substantially different to the curves calculated in this work which probably has arisen from the use of a squarewave filter function to degrade the high resolution data and may also account for part of the difference.

It would appear from the model comparisons made to date the discrepancy between the measured and calculated data for the two ranges 5.03 and 9.05 km can be confined to an absence of a significant contribution from the water contiuum absorption which to date has been neglected because it has been thought to be practically insignificant compared to the spectral absorption of H_2O and CO_2. This may not now be the case. Recent laboratory measurements by Burch and Gryvnak(ref.10) on the infra-red absorption by H_2O in the wings of the 6.3μm H_2O band indicate that self-broadened H_2O lines and to a lesser extent N_2-broadened H_2O lines absorb more significantly over a large portion of their wings than is assumed with Lorentz-shaped lines. Burch and Gryvnak even go as so far to say that the extra absorption in this region exceeds the total absorption by water near 10μm. If this is the case the extra absorption should exhibit a strong negative temperature dependance as is evident for the 8 to 12μm H_2O continuum absorption. Further laboratory work is needed to resolve the molecular absorption mechanisms in this region.

In the wavelength region 4.36 to 4.59μm (the 'red spike' region) agreement with the LOWTRAN3B data appears better (figures 10 and 11). While this at first sight suggests that the predicted absorbance arising from the wing of the strong CO_2 absorption band was well represented, no account has been taken of the effect of the tail of the spectral curve of filter 7 above the 4.59μm half-power point. (The half-power points for this filter were measured with two different spectrometers to better than 0.01μm). Because the atmospheric transmission near this region is significant, some IR radiation will be detected as a result of this tail and hence, the LOWTRAN3B model assuming a square wave filter would be incorrectly estimating the average transmittance. However, the average transmittance over this region is small and errors arising from integrating the absorbance curve and measuring the tail of the spectral curve for the filter become significant, which makes the predicted transmittance uncertain. A comparison between the LOWTRAN3B and HITRAN models for this region indicates that there is not good agreement in the shape of the wing of the CO_2 doublet;

$\tau_{LO}/\tau_{HI} \leq 1.5$ for ranges less than 9 km. However, for reasons given above this comparison probably is in error due to the use of an early version of the AFGL tape where a number of changes have since been made to the 4.3μm CO_2 absorption lines.

5.1.3 Transmission variation in 8 to 12μm spectral region

In this region the greatest uncertainty in transmission still arises from the water vapour continuum extinction coefficient as a function of precipitable water in the path, and temperature. A preliminary assessment has been made on the variability of the measured transmission data (for ranges 5 and 9 km) with precipitable water, obtained in the 8.2 to 11.8μm and 10.52 to 10.70μm wavelength regions for two visual range intervals. Data for the two regions are summarised in figures 12 to 15 where data are plotted for 3 temperature groups. Insufficient data were collected in the 8.33 to 9.80μm spectral region to allow any comment although the data have been included for the sake of completeness (figure 16). The following table indicates how the data (for all visual ranges) compare with LOWTRAN3B.

TABLE 3: SUMMARY OF THE MEASURED AND PREDICTED DATA FOR 8-12μm REGION

Wavelength Region	Range	
	5 km	9 km
8.2-11.8μm	Transmission data generally lower than LOWTRAN3B data.	Transmission data greater than LOWTRAN3B data for total precipitable H_2O > 90 mm
10.52-10.70μm	As Above	Moderate Agreement (NB: Number of data are small)

In the broadband region, the data indicate that as total precipitable water exceeds 90 mm LOWTRAN3B is over-estimating the transmission loss, while for the shorter range LOWTRAN3B is under-estimating the loss.

On the question of variation of transmission with temperature it does appear that the broad-band and narrow-band spectral region data for the 5 km path given in figures 12 to 15 are in closer agreement with the LOWTRAN3B data if a lower temperature was selected. A recent paper (Ref.11) has indicated that uncertainty still exists on the nature of the temperature dependance of the self-broadening coefficient (C_s^o) in the water continuum extinction coefficient (equ.1) and that the value of C_s^o used in LOWTRAN3B could be currently under-estimated. However, the measurements reported are not conclusive because of the small temperature range involved and the large scatter of the data within the 3 temperature groups.

5.2 Effect of visibility on transmission

To study the variability of the data with visibility a comparison was made between the measured transmission data and LOWTRAN3B using the maritime aerosol model with total particle numbers corresponding to visual ranges lying between 30 and 150 km (see figures 17 to 20). Data in the figures

indicate there is moderate agreement in the 1.5 to 2.5μm, 3.55 to 4.00μm and 4.36 to 4.59μm spectral regions over the 5 km pathlength. (Data points in the figures represent single measurements.) For the 9 km pathlength, LOWTRAN3B in the 3.55 to 4.00μm region appears again to overestimate the average transmission loss which may possibly be due to a lesser influence on the loss from the presence of water vapour (see Section 5.1.1) while for the 4.36 to 4.59μm region agreement remains moderate. Insufficient data were obtained over this path in the 1.5 to 2.5μm region to allow any assessment to be made. In the case of the 4.41 to 5.41μm region the large discrepancy due to water content (see Section 5.1.2) masks out any attempt to compare average transmission with visual range (see figure 20). Insufficient transmission data for relative humidities greater than 75% also ruled out the possibility of looking for growth effects on NaCl particles which would be the greatest contributor to the maritime aerosol at this site. No attempt was made to examine the variability of average transmission with visibility for filters 10 and 12 directly, because of insufficient data available for a particular precipitable water concentration interval. However, data have been rearranged to minimise the effects of water vapour concentration and temperature by making a relative comparison. The measured data from each region (for a given pathlength) are plotted (see figure 21) in the form $\tau_{10.52-10.70\mu m}$ versus $\tau_{8.2-11.8\mu m}$ for identical precipitable water concentrations. LOWTRAN3B predicts the relative variation of transmission with temperature in the 2 regions to move along a curve of constant visibility and any lateral displacement to the curve will be as the result of variation in visibility. Agreement with the predicted curve is good. Therefore, apart from any differences between the experimental and theoretical data due to precipitable water concentration and temperature the effect of visibility appears to be in line with the predicted variation.

5.3 Aerosol size distributions

During the present studies on IR transmission through the atmosphere, samples of the aerosol have been collected at the radiometer site on 7 occasions during transmission measurements. From the measurements made on three of these samples (collected on 0.05μm millipore filters for relative humidities < 70%) the distributions best fit a log normal distribution; the form of the equation being

$$n(r) = \frac{d\,N}{d(\log r)} = \frac{2.3\,N_T}{\sigma_z\sqrt{2\pi}} \exp\left\{\frac{-1}{2\sigma_z^2}\left(\ln\left(\frac{r}{r_m}\right)\right)^2\right\}$$

where $r_m = 0.3\mu m$ and $\sigma_z = 0.71$

An example of one of the distributions is given in figure 22. All samples have been collected where the prevailing winds over the ocean (for the velocity range 4-6 m/sec) originate well south of the measurement site and are not expected to have a very large continental component. Hence the maritime size distribution at present used in LOWTRAN3B may not be completely representative for some 'ocean-type' waters encountered in the Southern Hemisphere. However, the use of a bimodal size distribution may not be greatly in error because those particles which have radii less than 0.1μm and regarded as continental in nature are expected to be optically insignificant in the IR wavelength regions. Calculations will be made using an aerosol extinction model (which accepts any measured size distributions and complex refractive index data) to determine the precise effect small particles have on the extinction coefficient in the IR region.

6. CONCLUSIONS

This preliminary examination of the IR transmission data measured near the air-sea interface for 'ocean-type' waters in a temperate environment has indicated that agreement with LOWTRAN3B does not appear to be good in several spectral regions. In the 4.4 to 5.4μm region LOWTRAN3B is under-estimating the transmission loss for both ranges, which may be due to the absence of the water vapour continuum absorption spectrum. For long ranges in the 8 to 12μm region the model could be over-estimating the transmission loss as the precipitable water increases. Further, the variation of transmission loss with temperature appears to remain uncertain. Since an empirical expression is used for the temperature dependance of $C_s^o(\nu)$, further laboratory studies may be needed to refine the precise relationships of $C_s^o(\nu)$ and γ on temperature although the variation of γ with temperature may only be small.

The study so far has pointed to the fact that more transmission data are required to establish, with certainty, the reasons for these discrepancies which have appeared so far with LOWTRAN3B. To this end the measurement programme is to continue into 1979 to collect more transmission and meteorological data at the present coastal site. It is proposed to make measurements at a tropical site later. The present programme will also include aerosol sampling, and recording the visibility, temperature and relative humidity several metres above the water at locations along the path. These measurements will be made from a boat on different occasions when the appropriate winds are experienced. These data will be correlated with respective data obtained concurrently at each end of the path. Aerosol size distributions several metres above the sea surface could, in particular, exhibit a higher number of particles with radii greater than 5μm.

7. ACKNOWLEDGEMENTS

Acknowledgement is made to the District Council of Victor Harbor and to the Department of Marine and Harbors for providing operating sites on Granite Island and The Bluff, and for the use of the causeway to gain access to Granite Island. The author and his Laboratory appreciate greatly the co-operation received.

NOTATION

α	scanned filter area
f	flow rate
$n(r)$	particle number density/log radius interval
r	particle radius
r_m	particle modal radius
t	sampling time
A	filter area
C_s^o	self-broadening water absorption coefficient
N	cumulative particle number density
N_T	total number of particles/cm^3
P_{H_2O}	partial pressure of atmospheric water vapour
P_T	total atmospheric pressure
R	range
T	absolute temperature
T	atmospheric transmission
γ	N_2-H_2O relative broadening absorption coefficient
λ	wavelength
ν	frequency
ρ	precipitable water
σ	extinction coefficient
σ_z	log-normal standard deviation
ω	absolute humidity

REFERENCES

No.	Author	Title
1	J.E.A. Selby and R.A. McClatchey	"Atmospheric Transmittance From 0.25 To 28.5μm: Computer Code LOWTRAN3." AFCRL-TR-75-0255, May 1975.
2	D.R. Cutten	"Instrumentation For Investigating The Propagation of Infra-red Radiation Over Long Atmospheric Paths." WRE-Technical Report 1889(A), 1978.
3	D.R. Cutten et al	"A Visibility Meter For Monitoring Atmospheric Aerosol Parameters." Atmospheric Environment, Vol.9, Page 253, 1975.
4	O. White et al	"Water Vapor Continuum Absorption In The 3.5-4.0μm Region." Applied Optics, Vol.17, Page 2711, 1978.
5	D.E. Burch, D.A. Gryvnak and J.D. Pembrook	"Investigation Of The Absorption Of Infrared Radiation By Atmospheric Gases: Water, Nitrogen, Nitrous Oxide." Philco-Ford Aeronutronic Division Report U-4784, (AFCRL-71-0124), January 1974.
6	J.A. Dowling et al	"High Resolution Field Measurement Of Atmospheric Transmission." Proceedings SPIE, Vol.142, Page 25, 1978.
7	H.W. Yates and J.H. Taylor	"IR Transmission Of The Atmosphere." NRL Report 5453, 1960.
8	K.M. Haught and D.M. Cordray	"Long-path High Resolution Atmospheric Transmission Measurements: Comparison With LOWTRAN3B Predictions." Applied Optics, Vol.17, Page 2668, 1978.
9	T.W. Tuer	"Thermal Imaging Systems' Relative Performance: 3-5μm vs 8-12μm." Technical Report AFAL-TR-76-217, January 1977.
10	D.E. Burch and D.A. Gryvnak	"Laboratory Measurements Of The Infrared Absorption By H_2O and CO_2 In Regions Of Weak Absorption." Proceedings SPIE, Vol.142, Page 16, 1978.
11	G.P. Montgomery	"Temperature Dependance Of IR Absorption By The Water Vapor Continuum Near 1200cm^{-1}." Applied Optics, Vol.17, Page 2299, 1978.

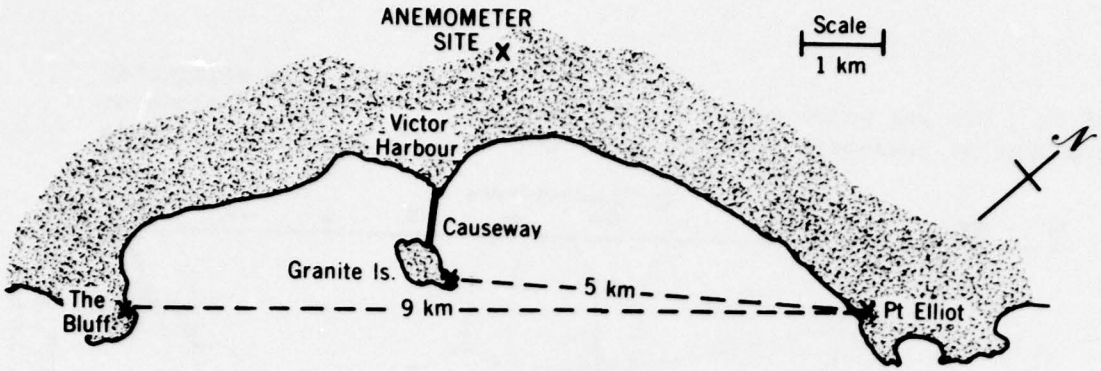

ELEVATION
(Not to scale)

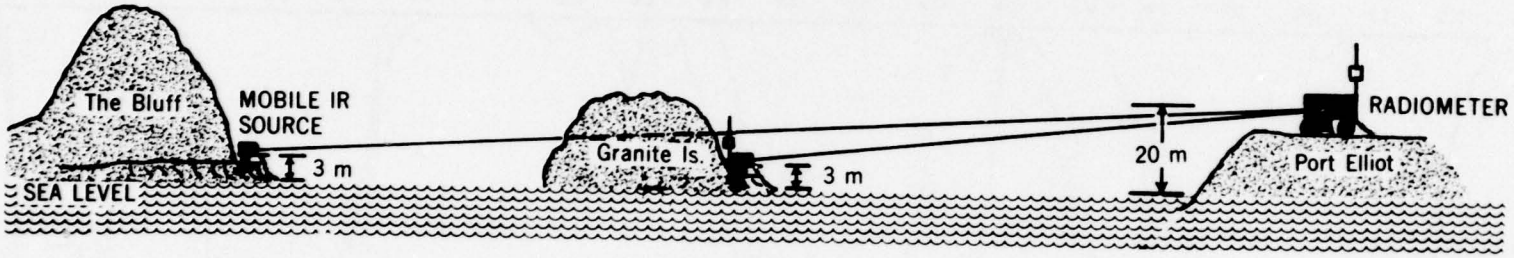

Figure 1. Transmission measurement site at Victor Harbor

ERL-0063-TM
FIGURE 1

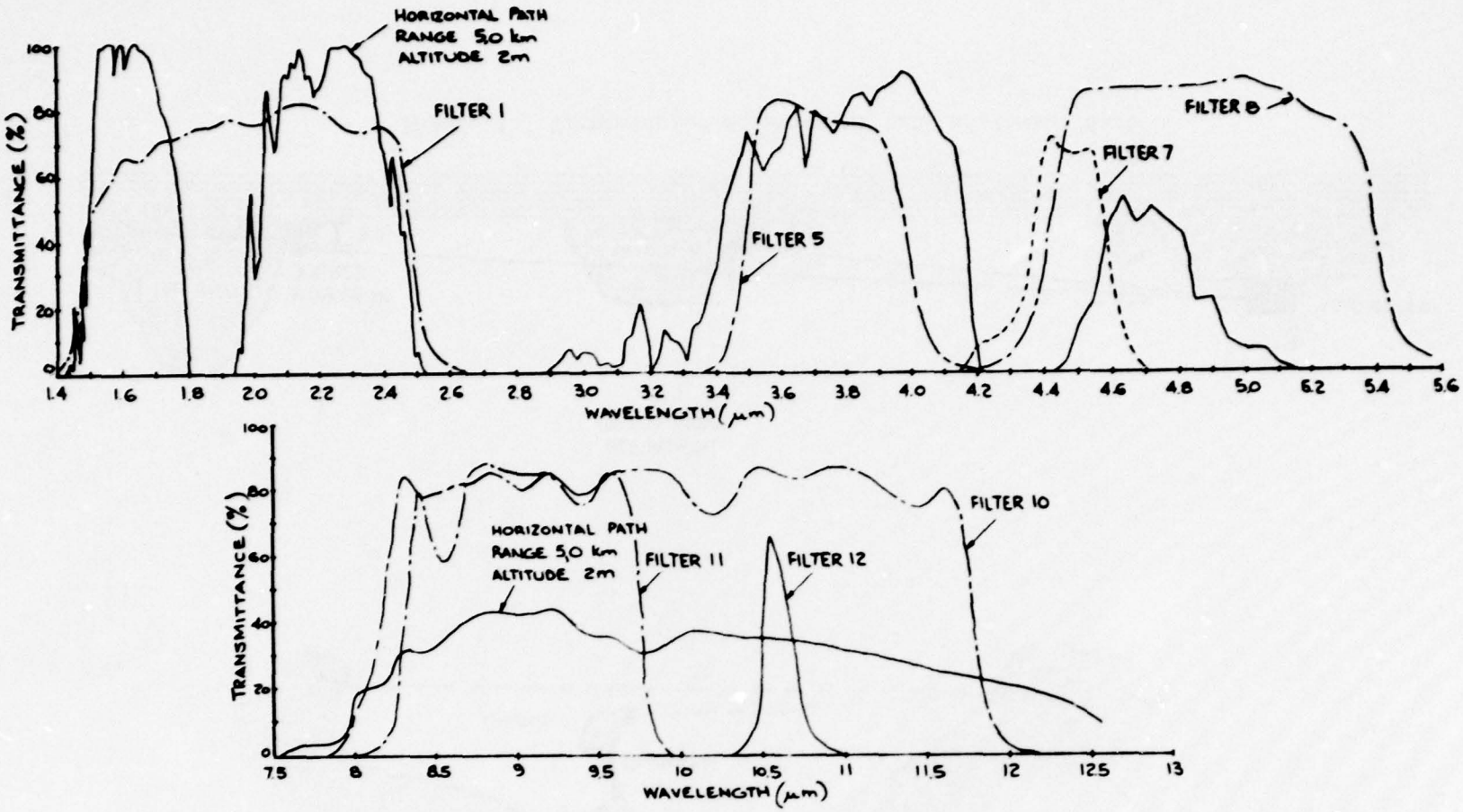

Figure 2. Spectral curves of filters used to define the broad-band IR transmission measurement regions. (The atmospheric transmission for the 5 km path is calculated from LOWTRAN 3B)

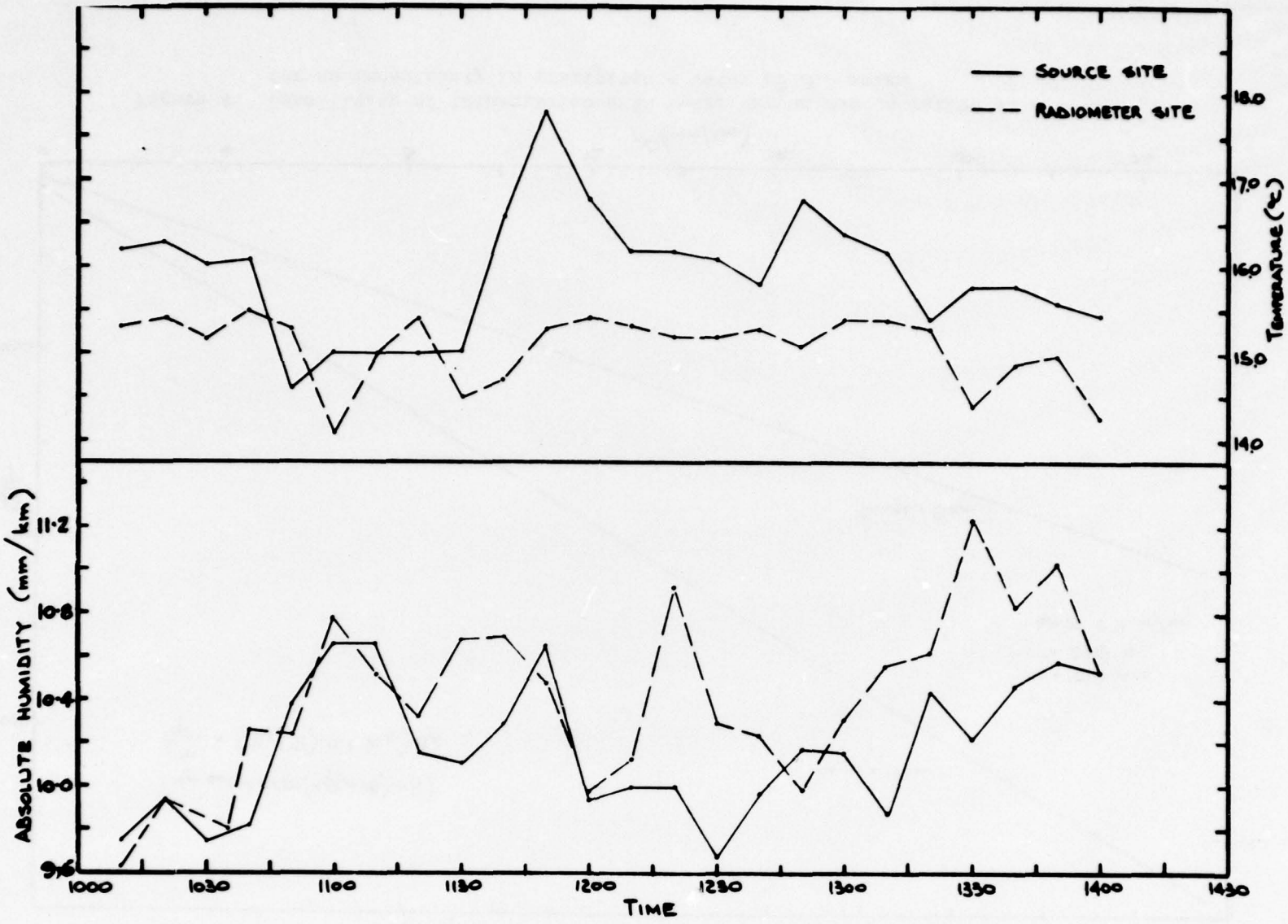

Figure 3. Absolute humidity and dry temperature measurements for each end of the 9 km path at Victor Harbor on 19 April 1978

ERL-0063-TM
FIGURE 3

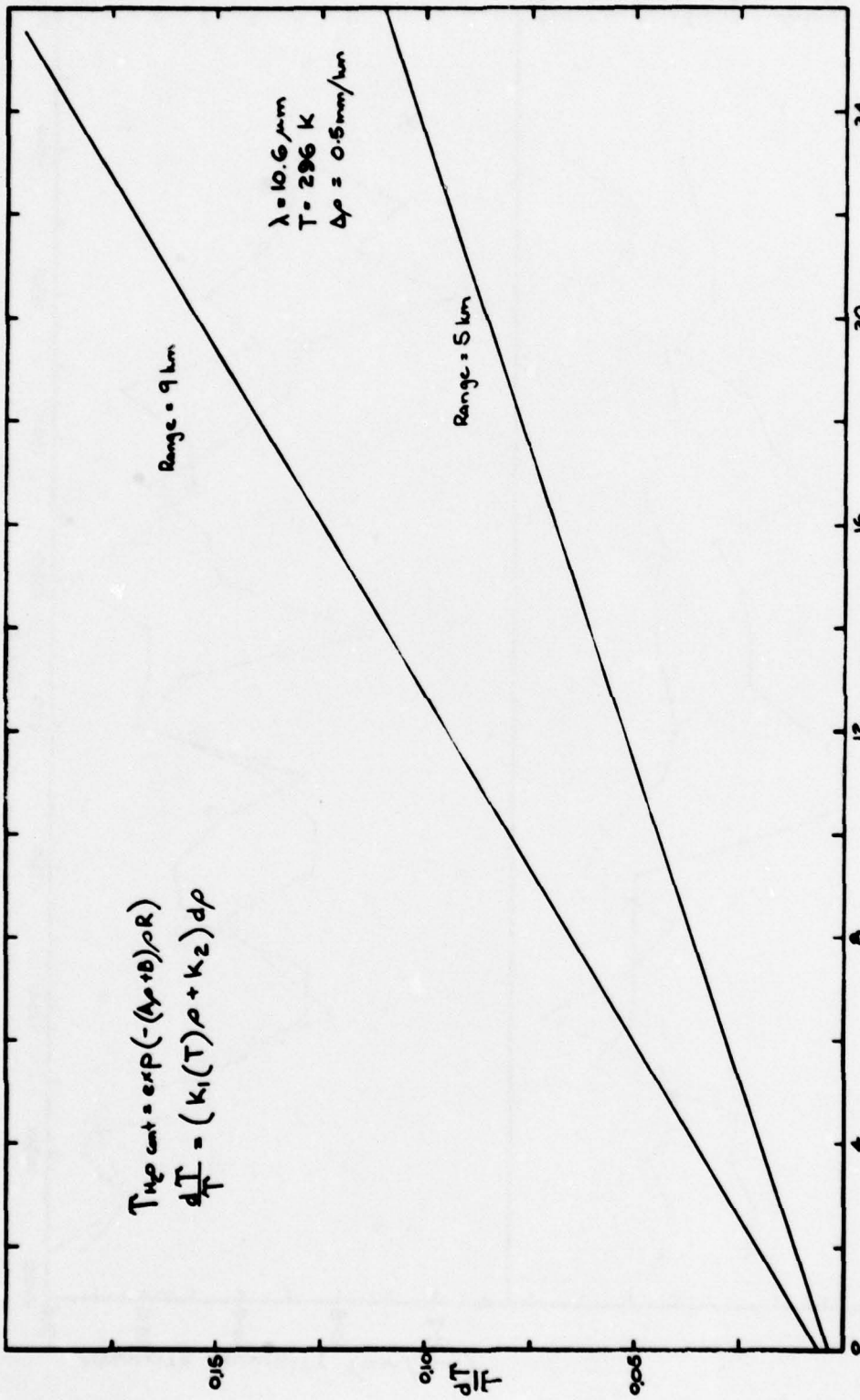

Figure 4. Sensitivity of transmission with water vapour concentration at λ = 10.6 μm for an uncertainty in precipitable water of 0.5 mm/km

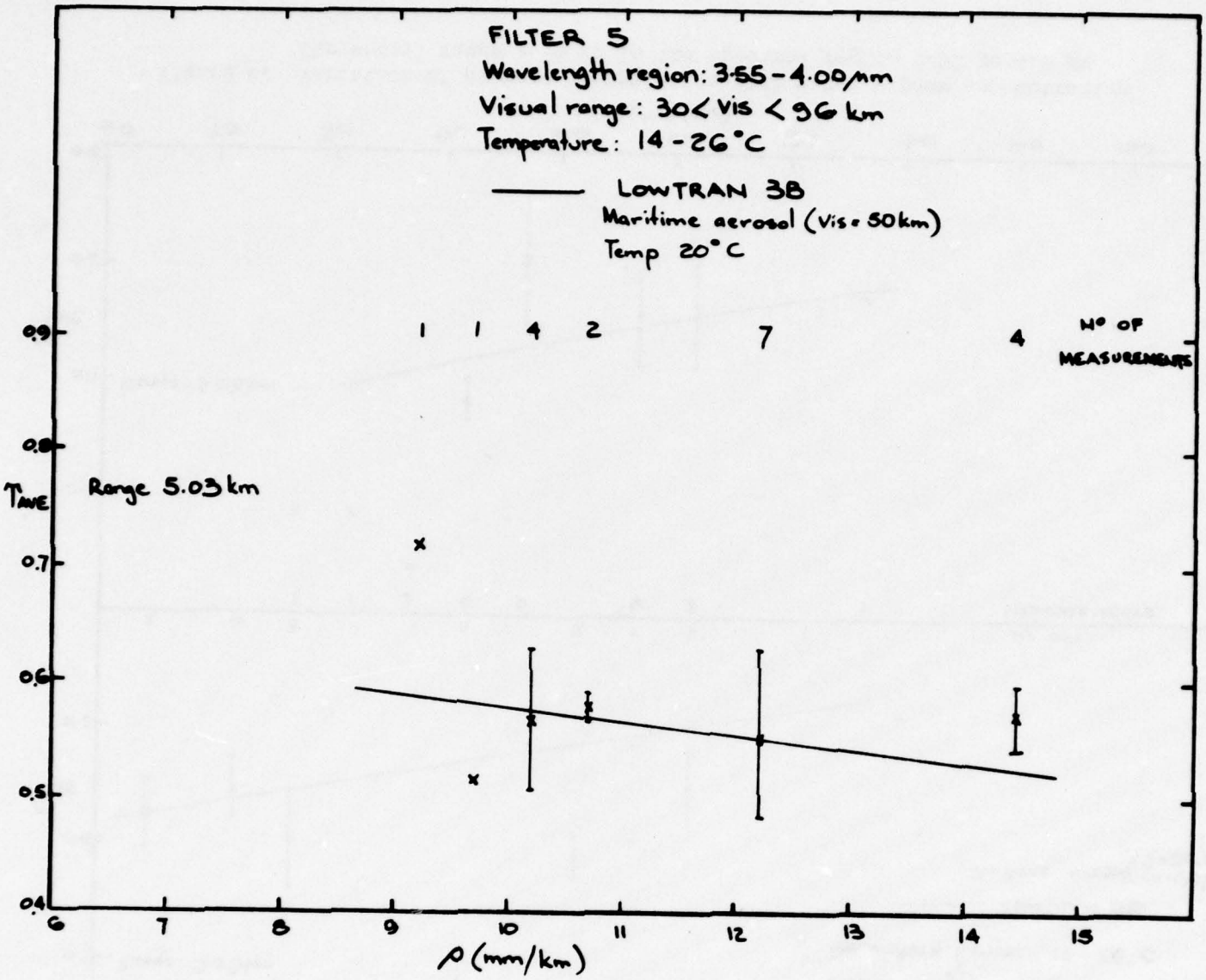

Figure 5. Variation of average transmission with water vapour concentration for visual range < 96 km in the spectral region 3.55 to 4.00 μm

ERL-0063-TM
FIGURE 5

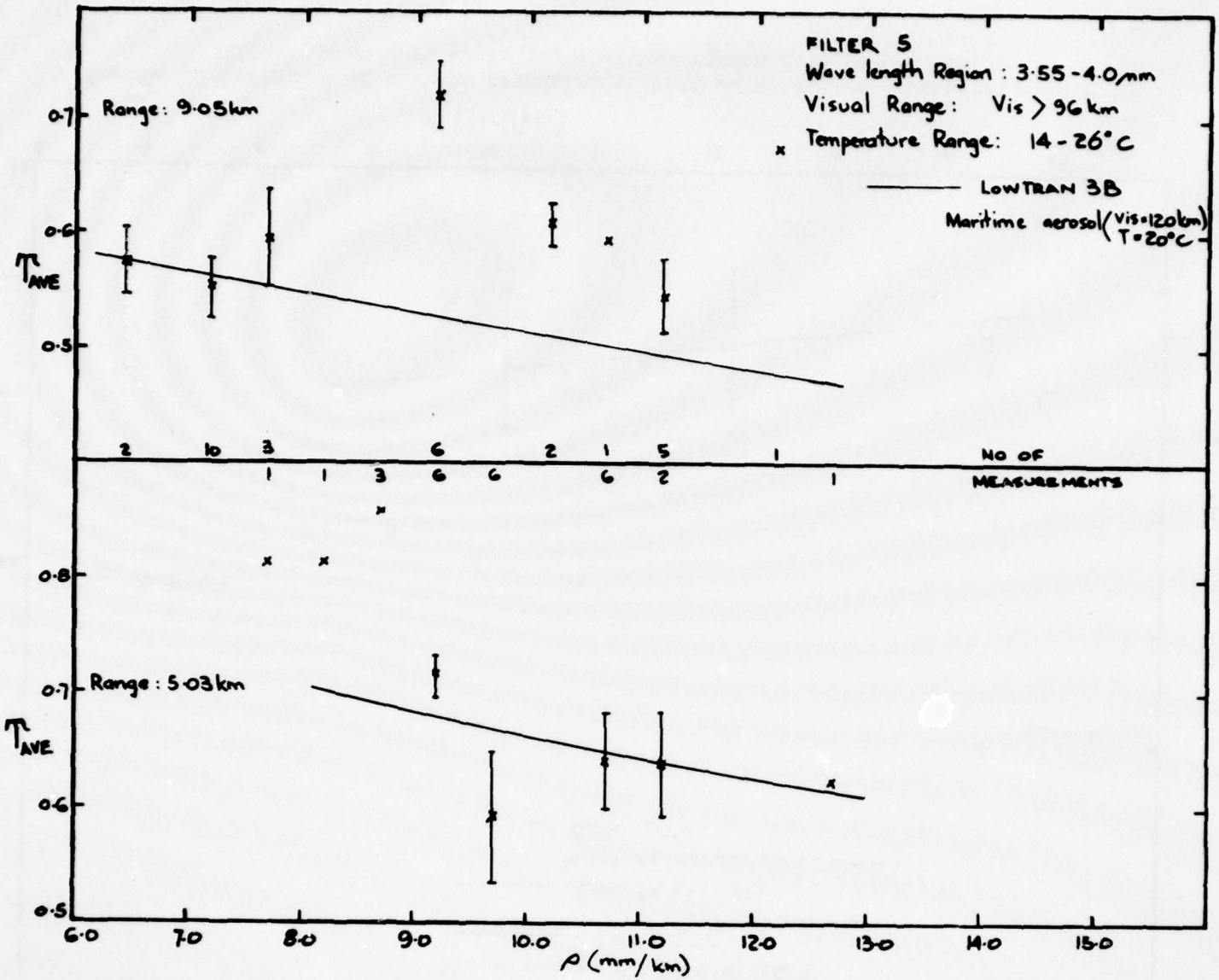

Figure 6. Variation of average transmission with water vapour concentration for visual range > 96 km in the spectral region 3.55 to 4.0 μm

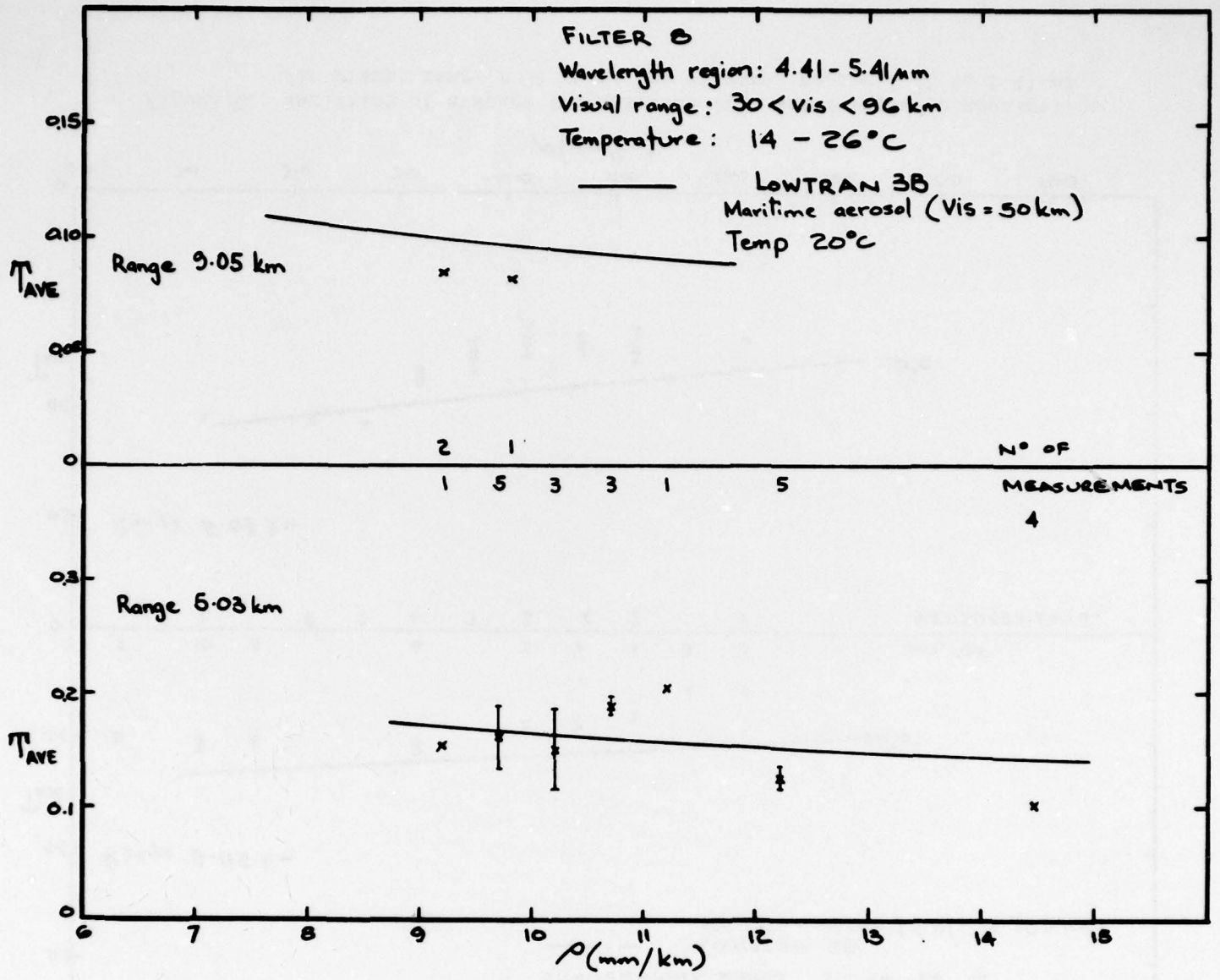

Figure 7. Variation of average transmission with water vapour concentration for visual range < 96 km in the spectral region 4.41 to 5.41 μm

FIGURE 7

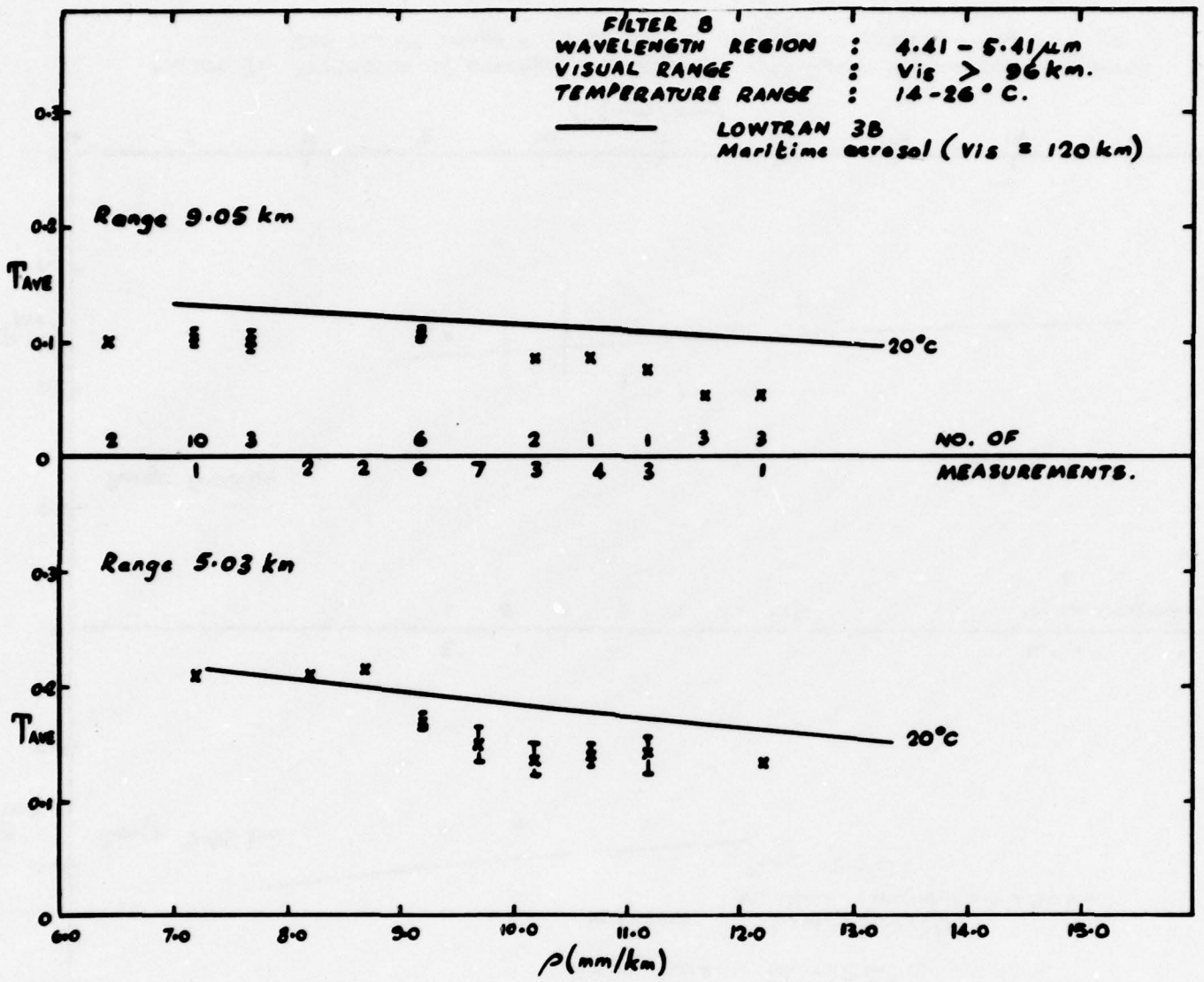

Figure 8. Variation of average transmission with water vapour concentration for visual range > 96 km in the spectral region 4.41 to 5.41 μm

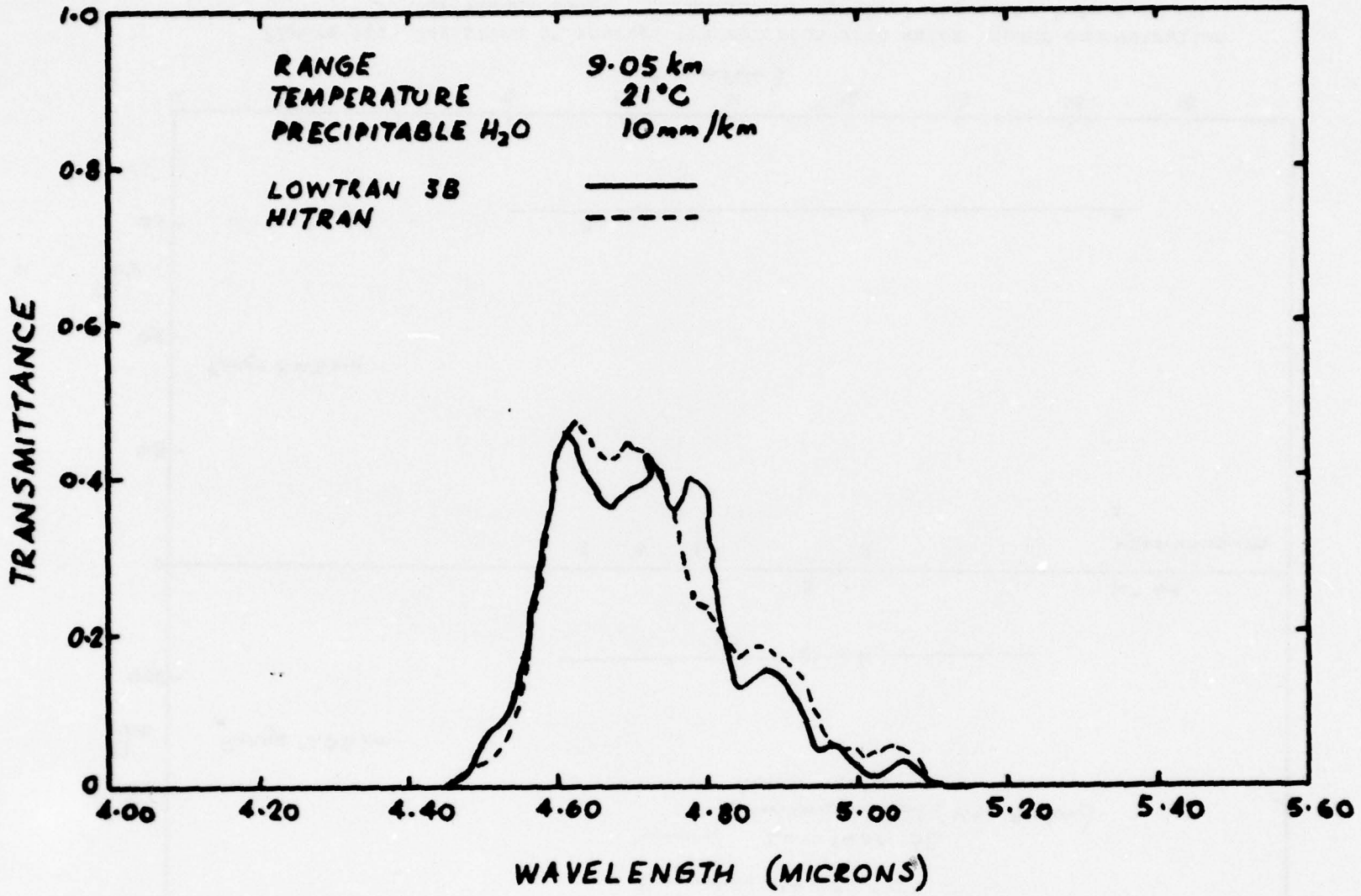

Figure 9. Comparison of LOWTRAN 3B and HITRAN IR spectra over 4.4 to 5.4 μm spectral region

ERL-0093-ATR
FIGURE 9

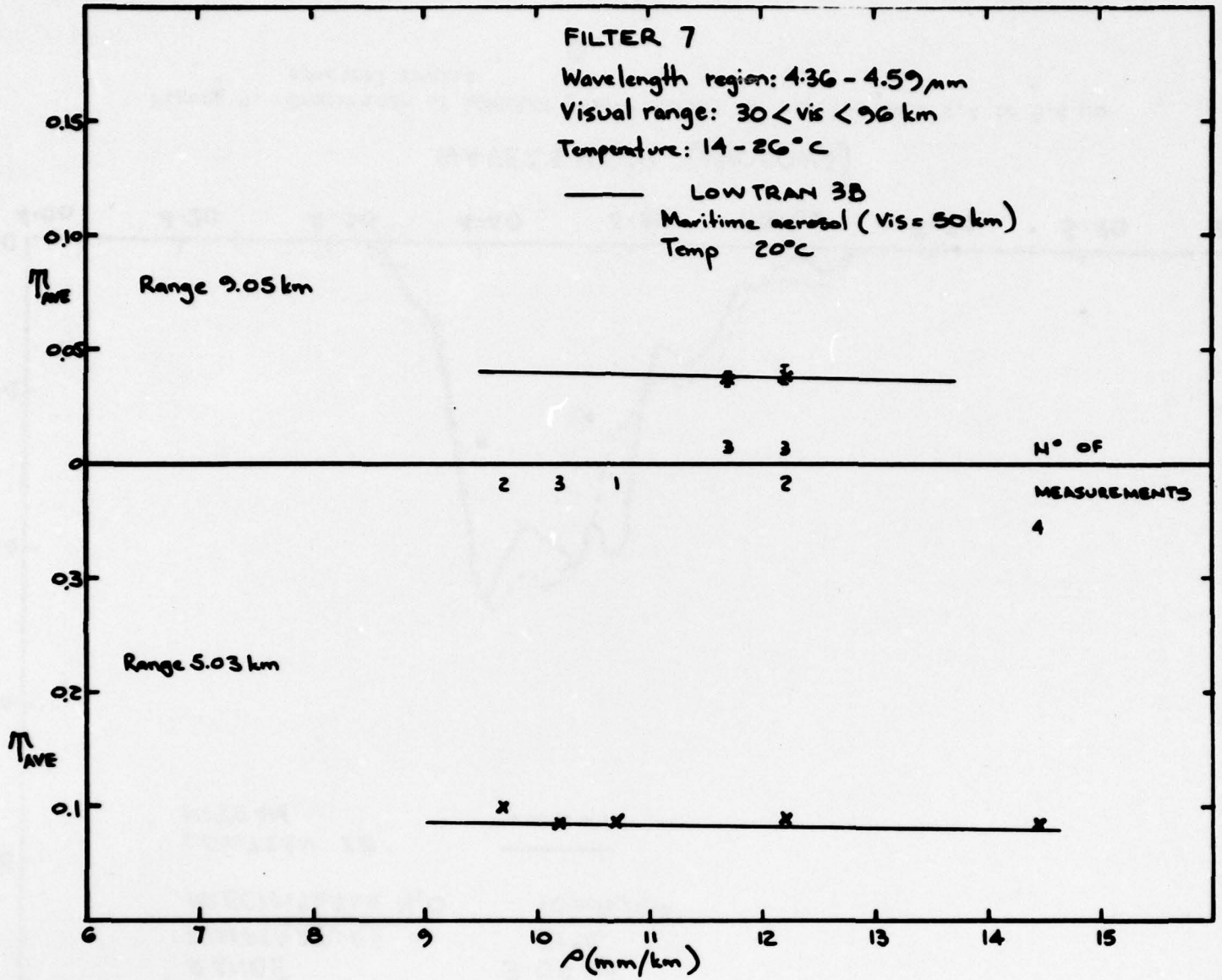

Figure 10. Variation of average transmission with water vapour concentration for visual range < 96 km in the spectral region 4.36 to 4.59 μm

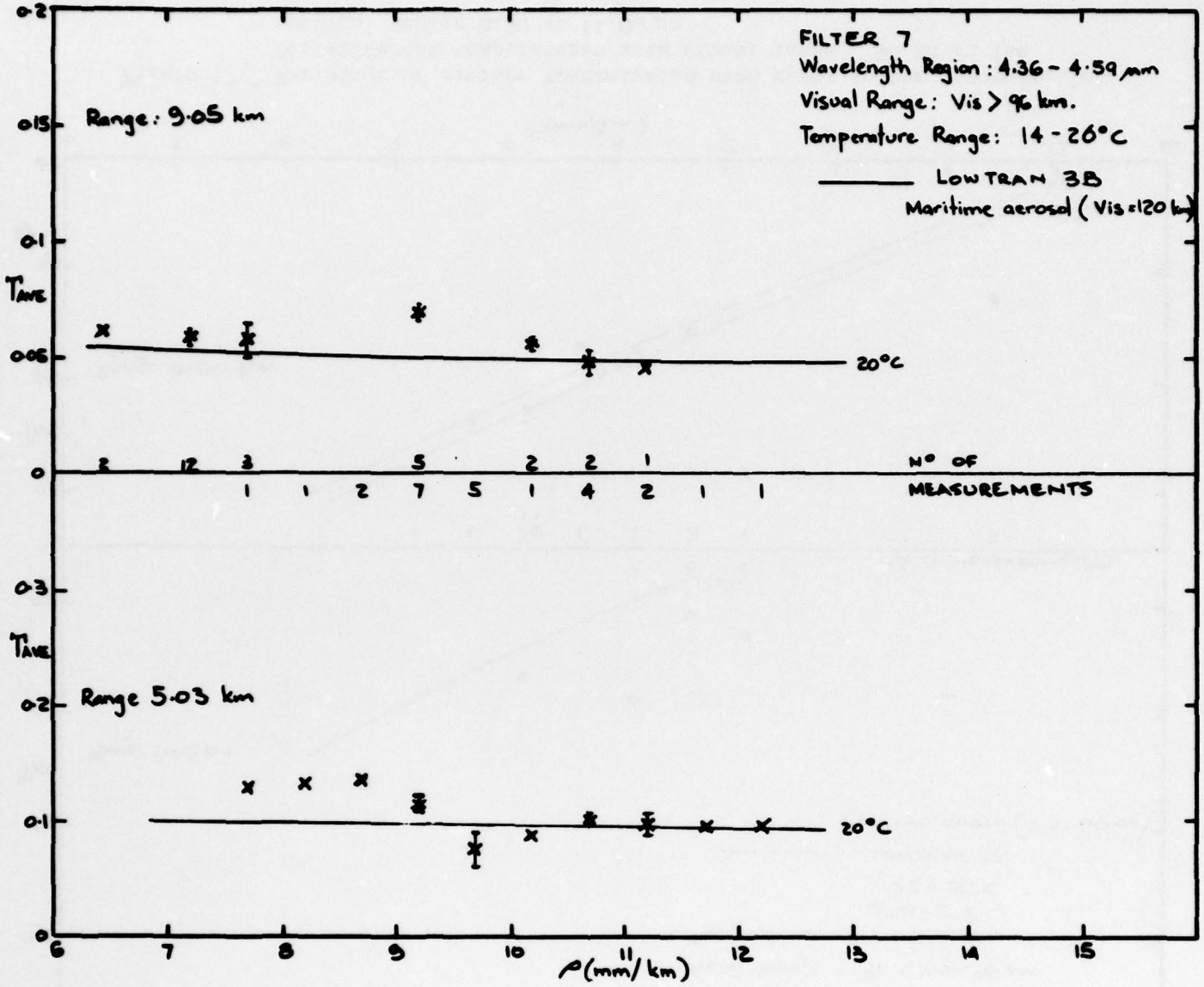

Figure 11. Variation of average transmission with water vapour concentration for visual range > 96 km in the spectral region 4.36 to 4.59 μm

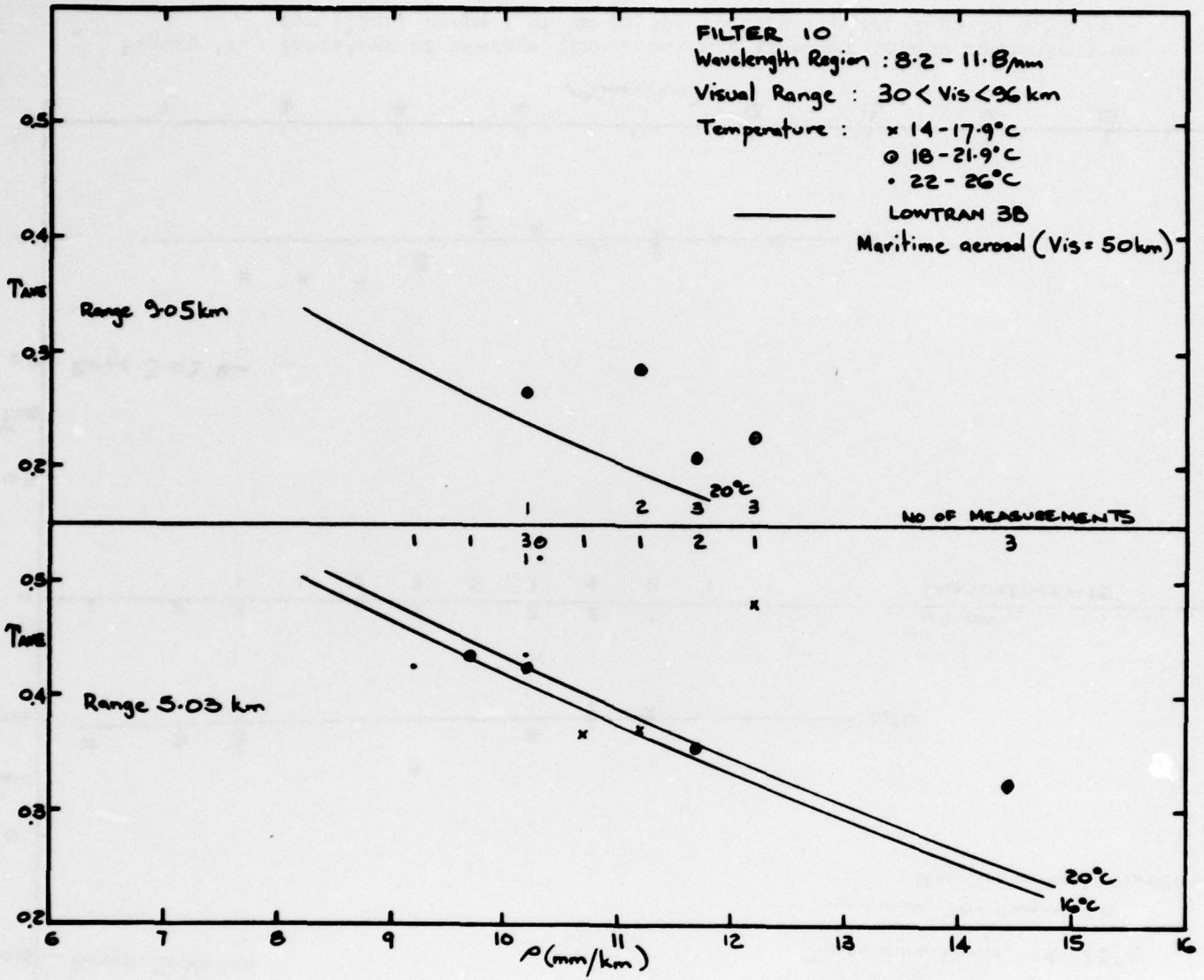

Figure 12. Variation of average transmission with water vapour concentration for different temperatures with visual range < 96 km in the spectral region 8.20 to 11.80 μm

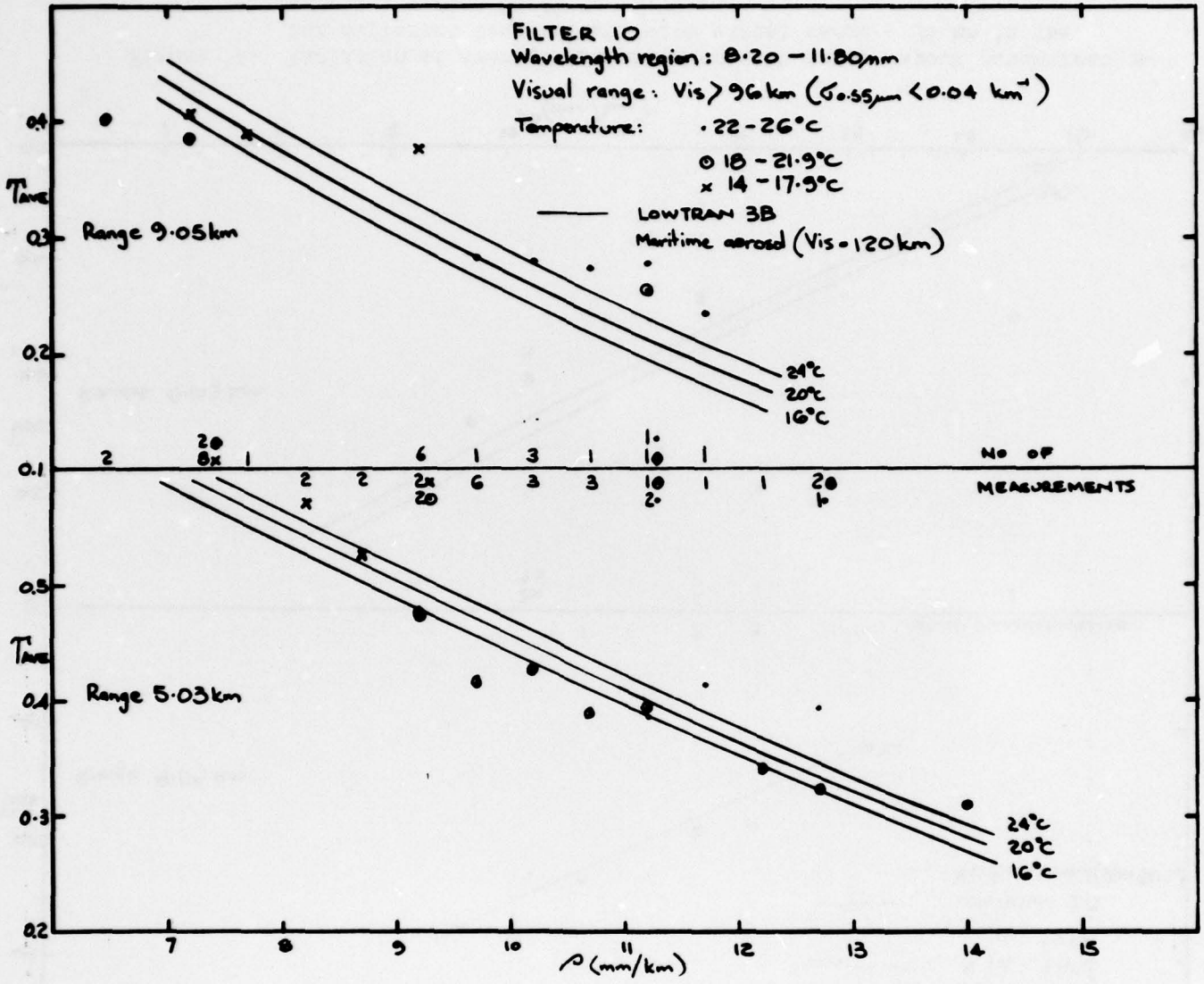

Figure 13. Variation of average transmission with water vapour concentration for different temperatures with visual range > 96 km in the spectral region 8.20 to 11.80 μm

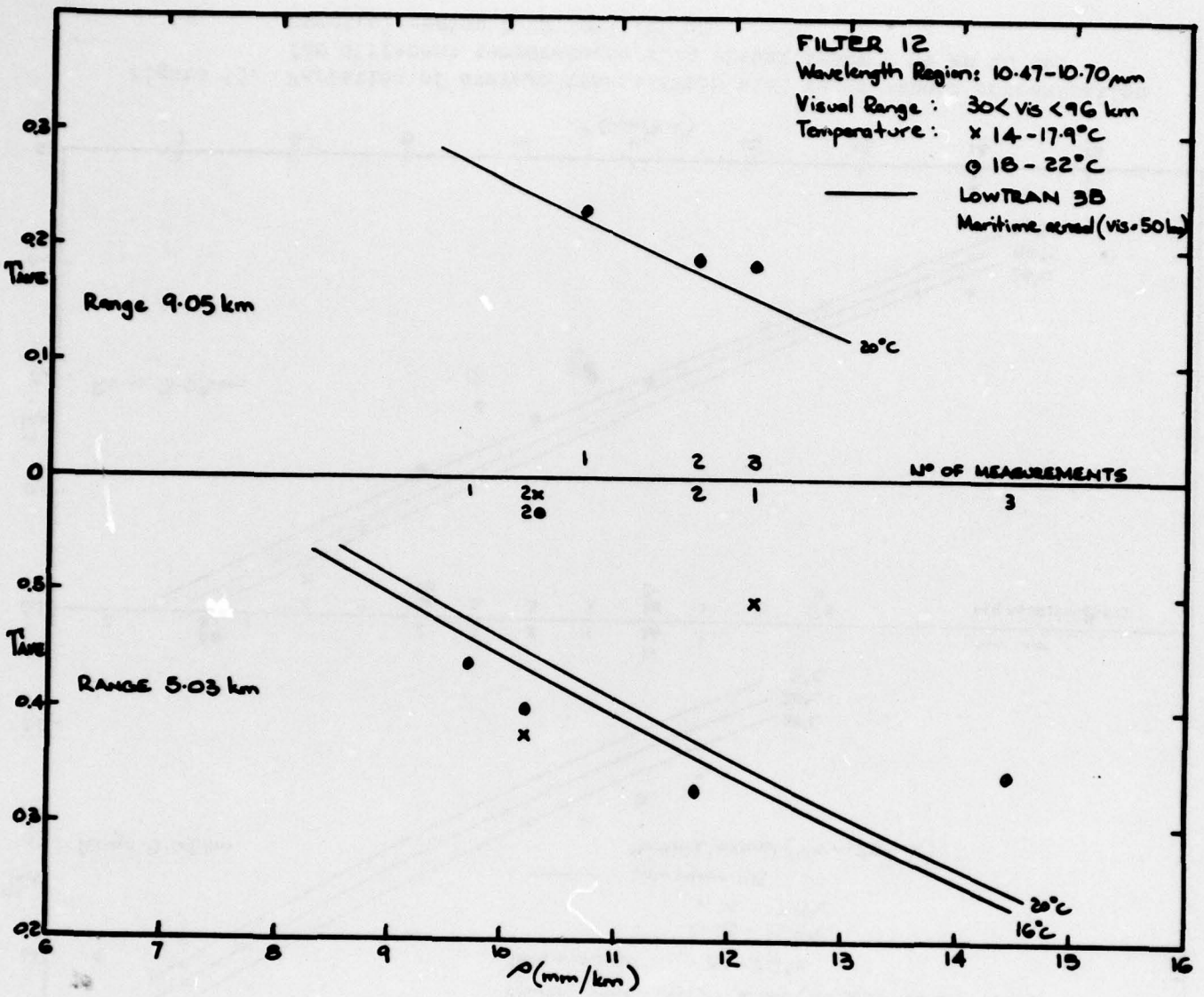

Figure 14. Variation of average transmission with water vapour concentration for different temperatures with visual range < 96 km in the spectral region 10.47 to 10.70 μm

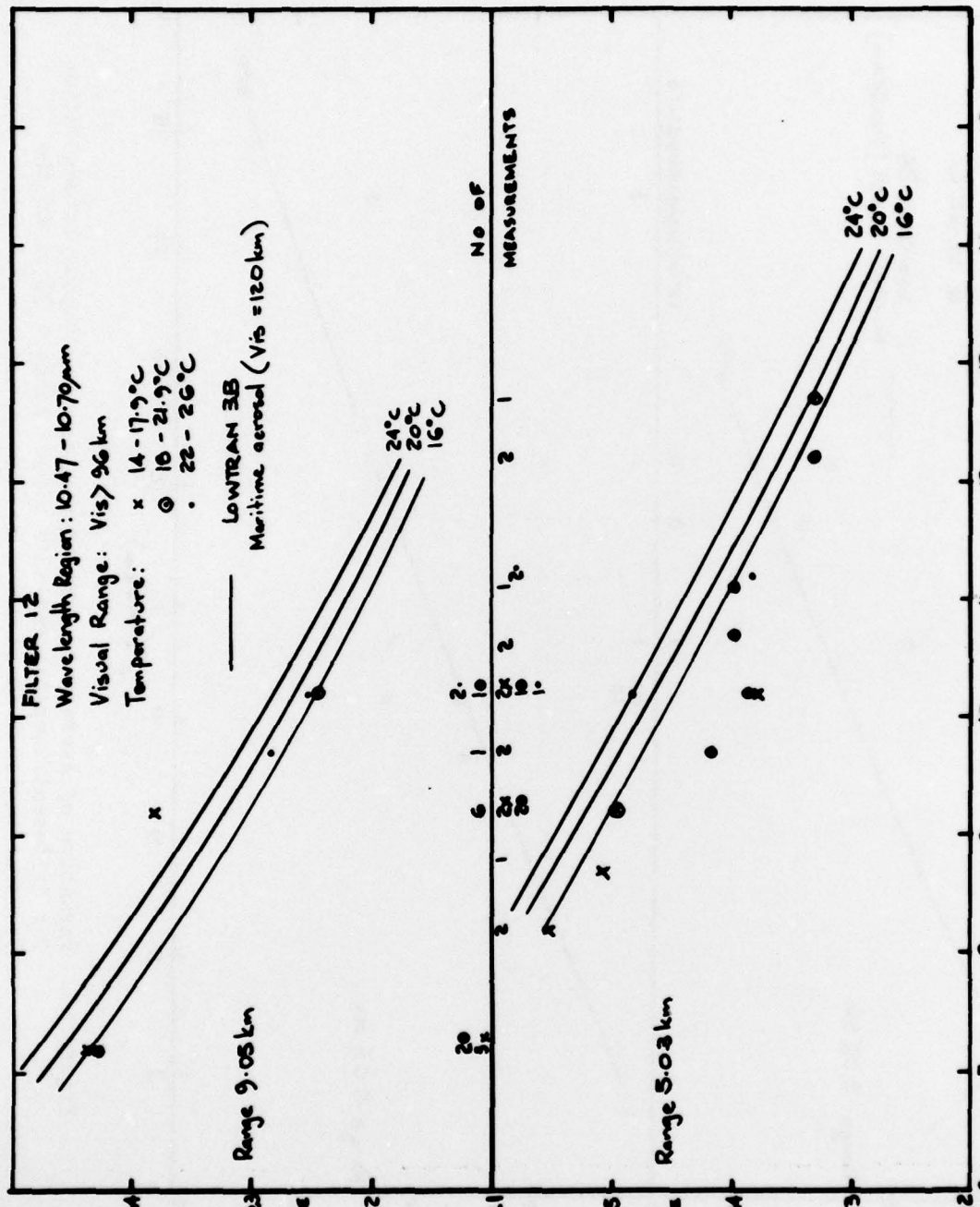

Figure 15. Variation of average transmission with water vapour concentration for different temperatures with visual range > 96 km in the spectral region 10.47 to 10.70 μm

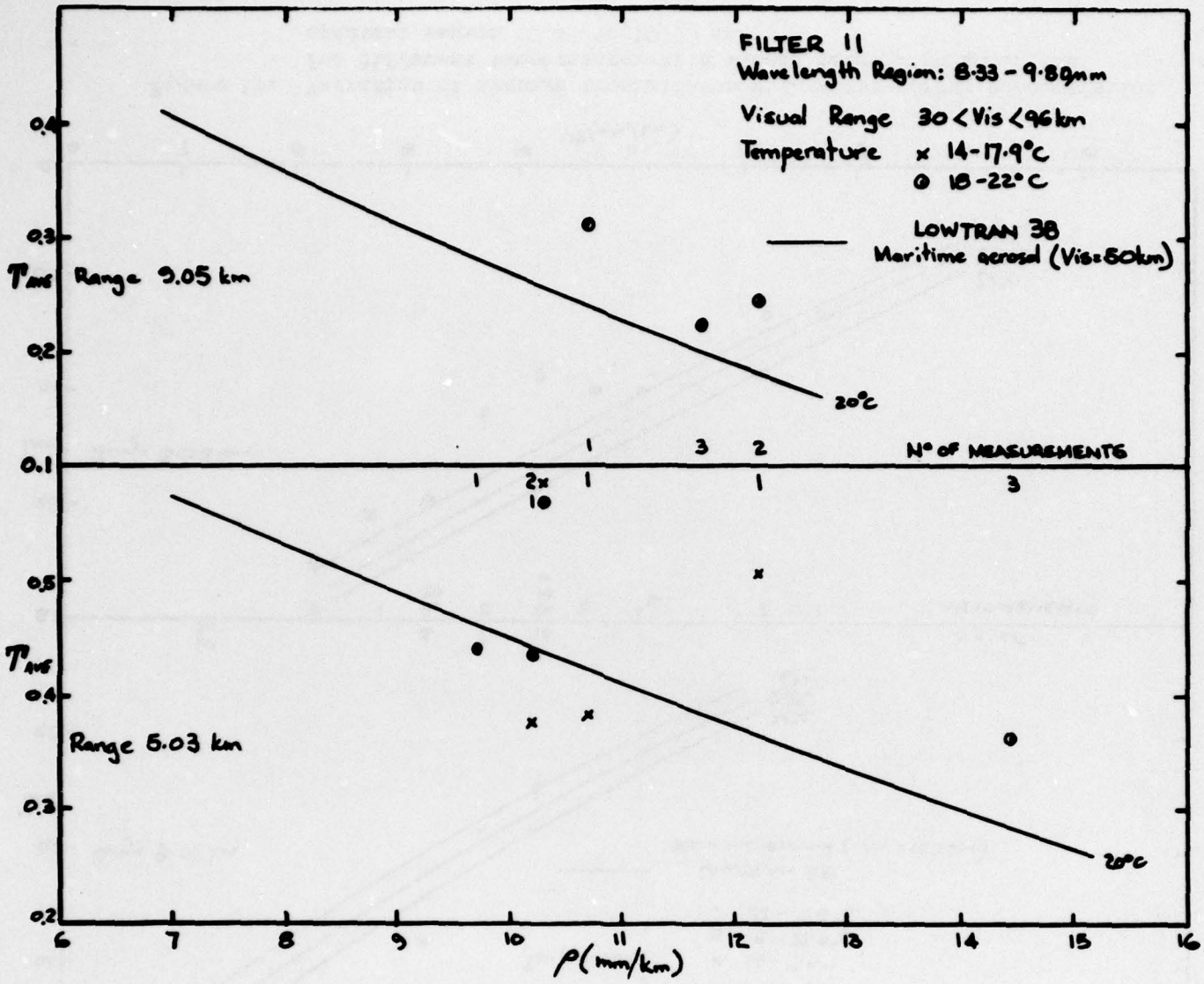

Figure 16. Variation of average transmission with water vapour concentration for different temperatures with visual range < 96 km in the spectral region 8.33 to 9.80 μm

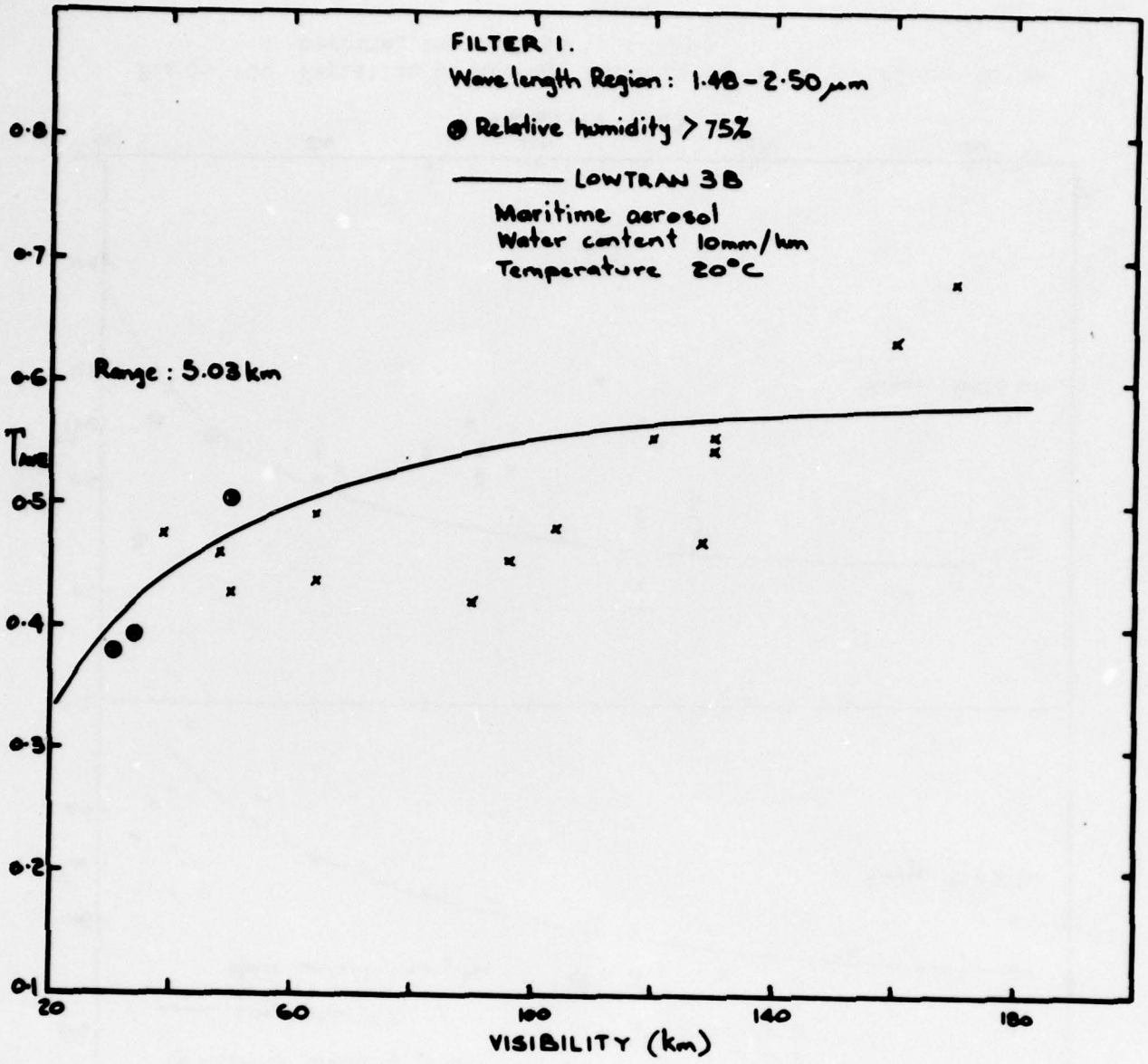

Figure 17. Variation of average transmission with visibility in the spectral region 1.48 to 2.50 μm

ERL-0063-TM
FIGURE 17

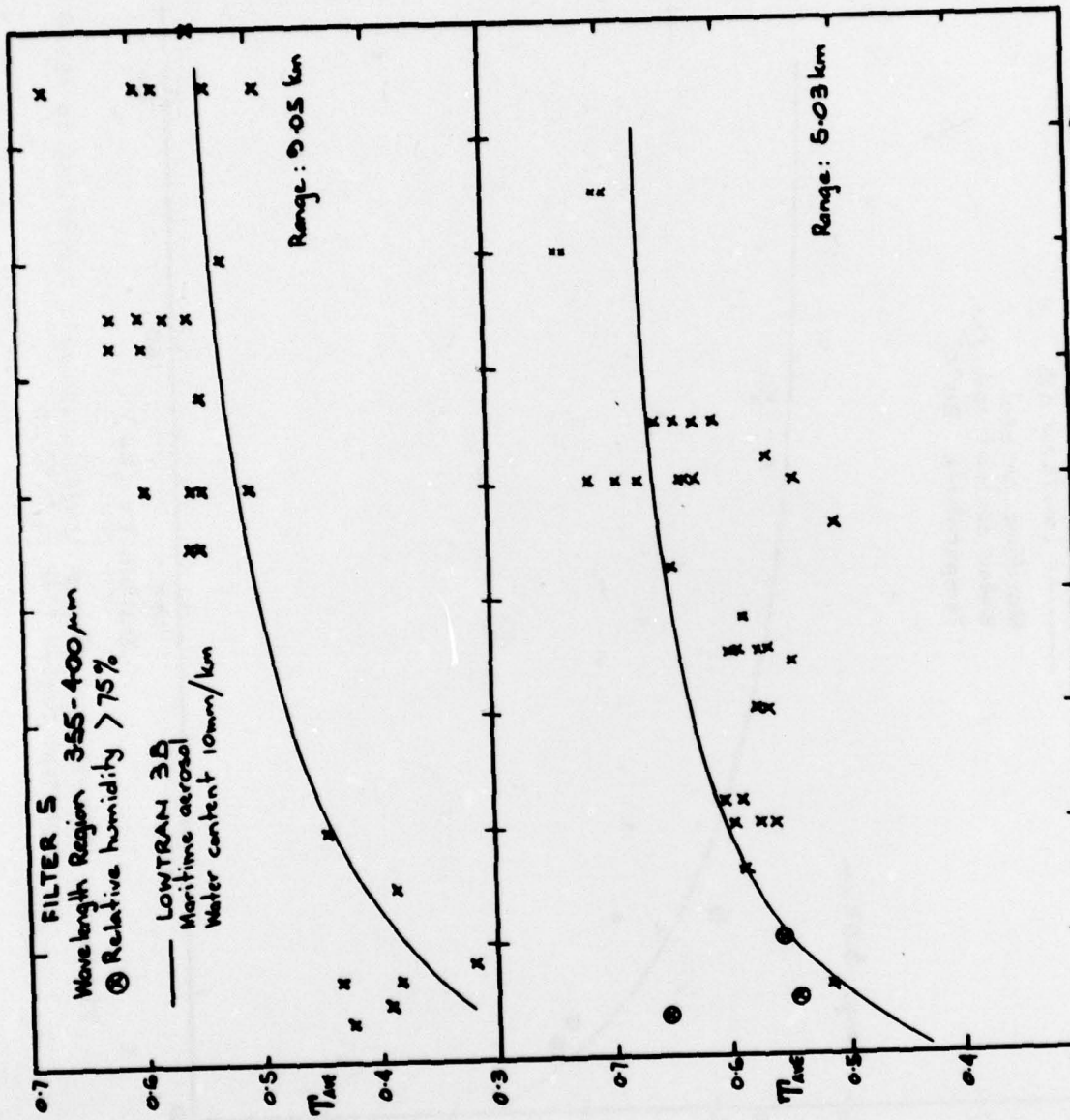

Figure 18. Variation of average transmission with visibility in the spectral region 3.55 to 4.00 μm

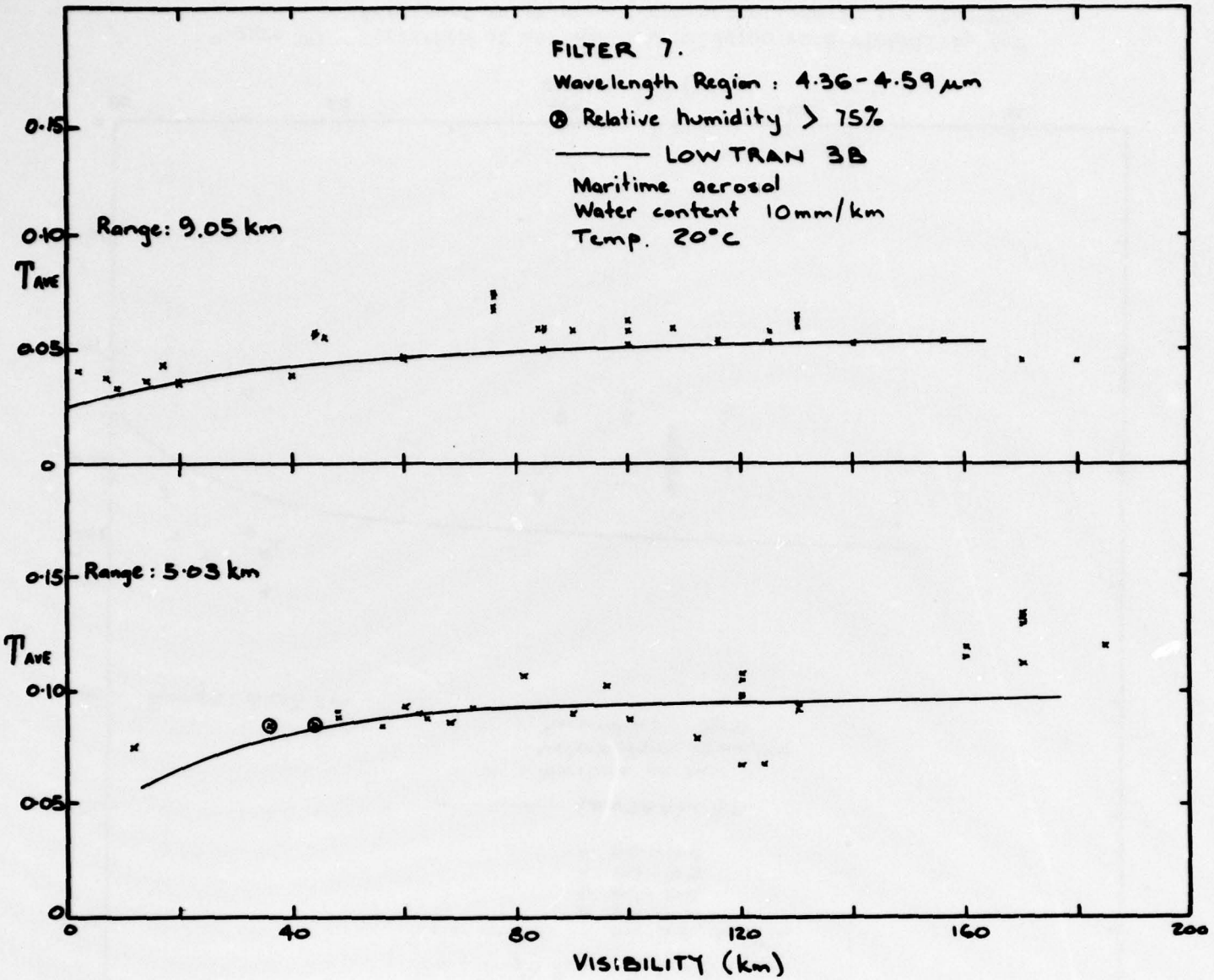

Figure 19. Variation of average transmission with visibility in the spectral region 4.36 to 4.59 μm

ERL-0063-TM
FIGURE 19

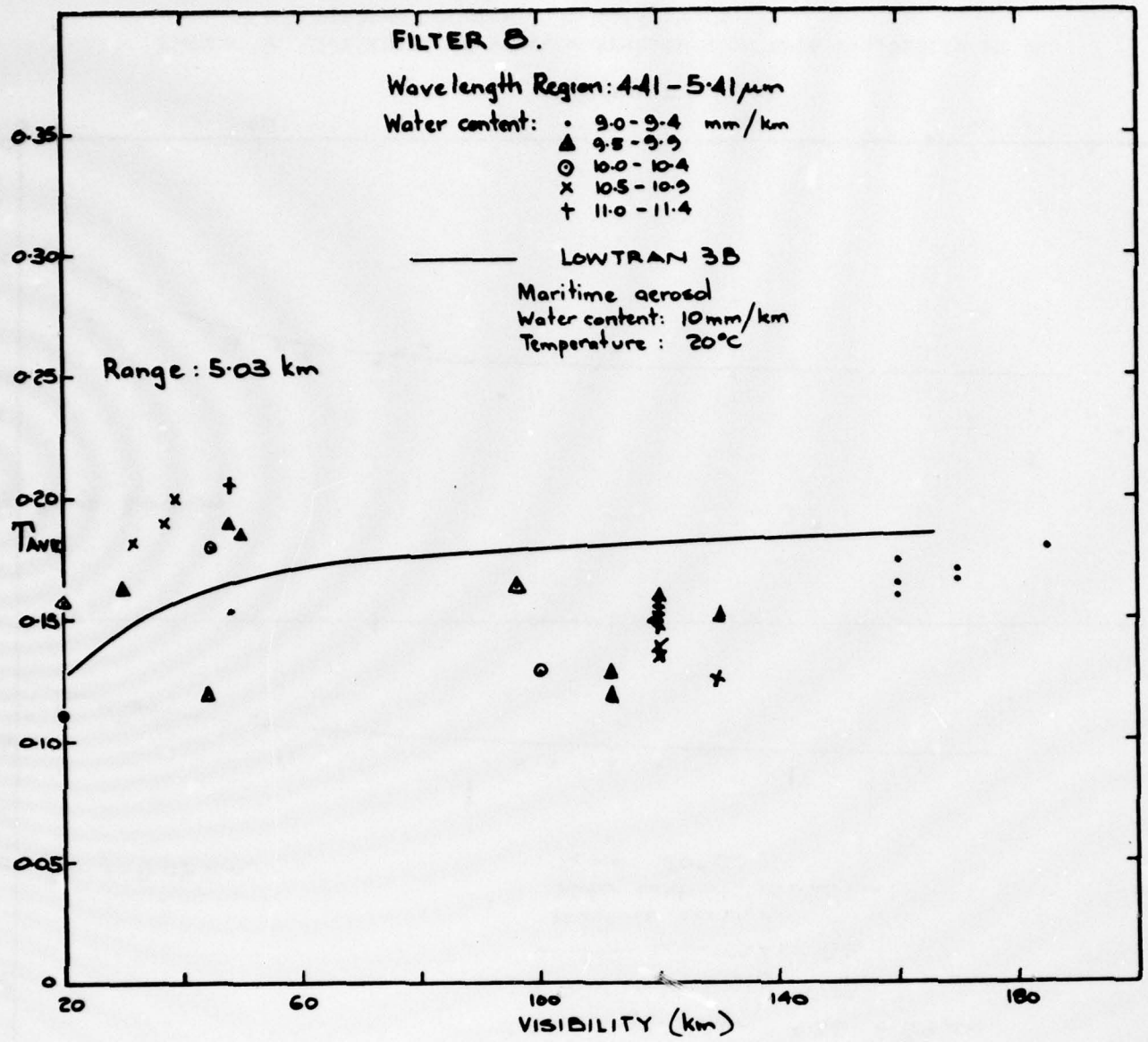

Figure 20. Variation of average transmission with visibility for different water vapour concentrations in the spectral region 4.41 to 5.41 μm

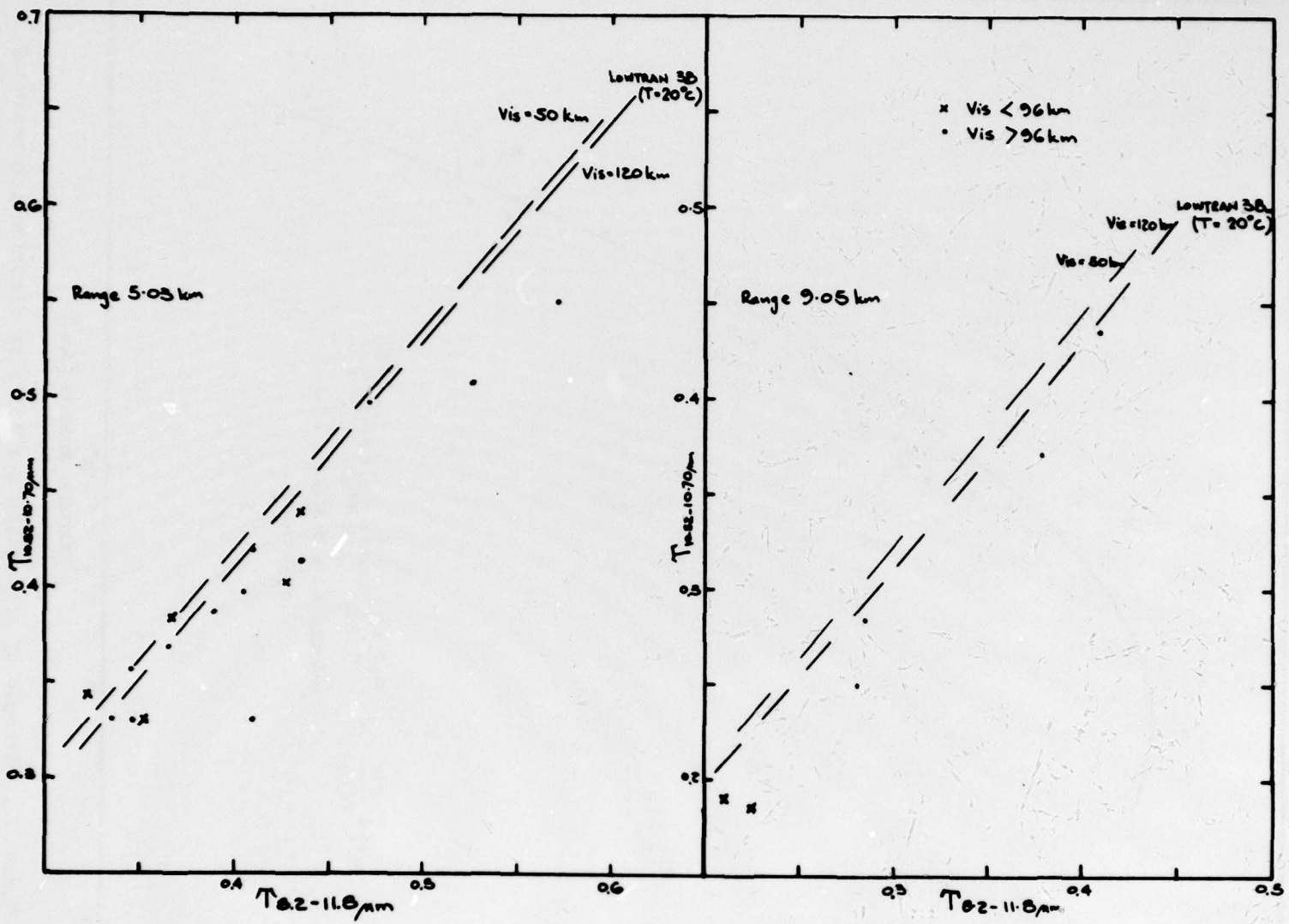

Figure 21. Comparison of average transmissions measured over a given path length in the 8.2 to 11.8 μm and 10.52 to 10.70 μm spectral regions with LOWTRAN 3B. Data are plotted for a given water vapour concentration at all temperatures

ERL-0063-TM
FIGURE 21

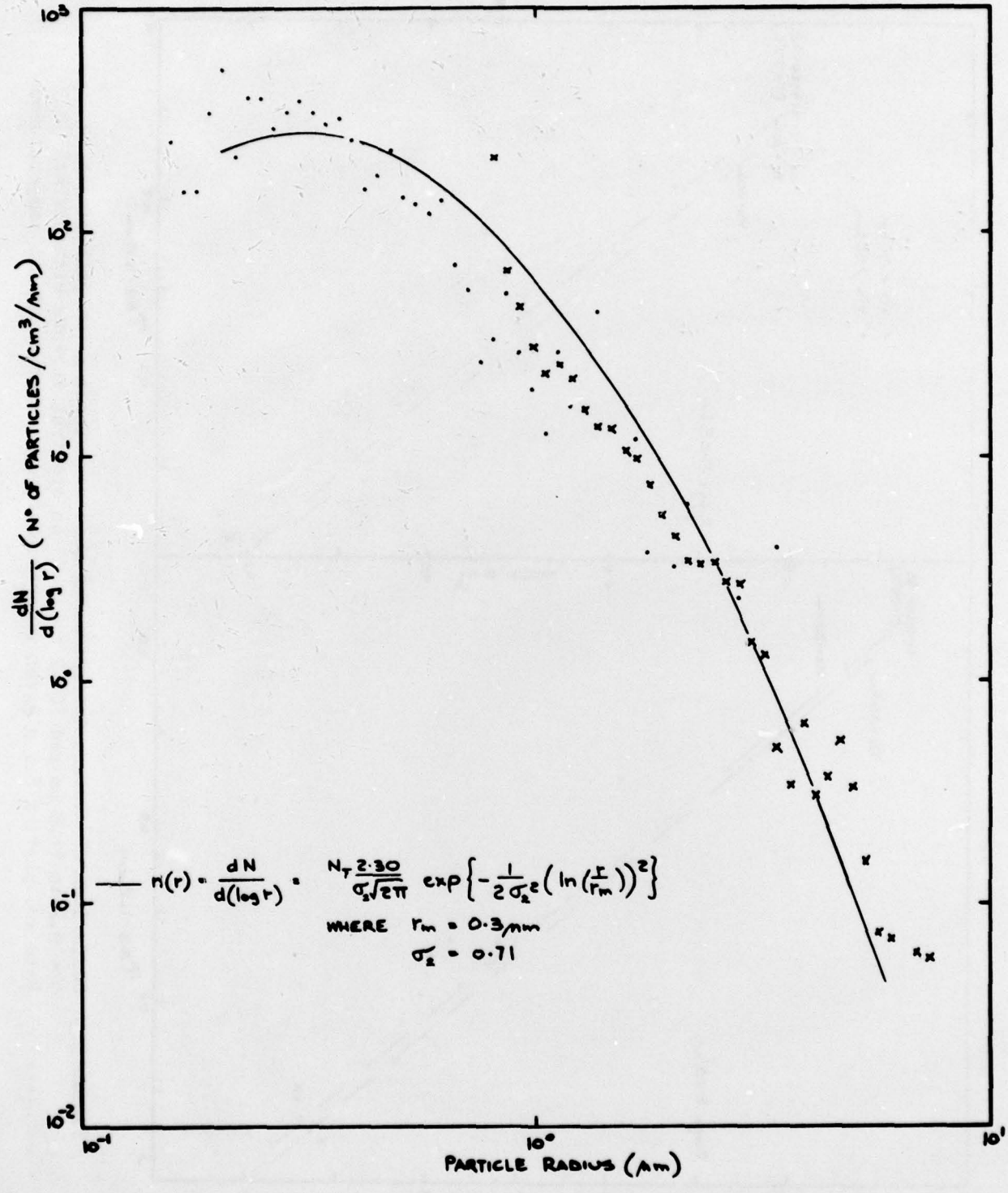

Figure 22. Example of a maritime aerosol size distribution measured at Victor Harbor on a day where the visual range was 60 km

DISTRIBUTION

EXTERNAL	Copy No.
In United Kingdom	
Defence Scientific and Technical Representative, London	1
Dr W.A. Shand, R.S.R.E.(C), Christchurch, Dorset	2
In United States	
Counsellor, Defence Science, Washington (Attention: M. Busch)	3
Dr P.B. Ulrich, Optical Sciences Division, Naval Research Laboratories, Washington	4
Dr J.S. Garing, Optical Physics Division, Air Force Geophysics Laboratory, Hanscom Air Force Base, Massachusetts	5
In Canada	
Mr G.A. Morley, Electro Optics Division, Defence Research Establishment Valcartier	6
In Australia	
Chief Defence Scientist	7
Deputy Chief Defence Scientist	8
Superintendent, Science and Technology Programs	9
Controller, Service and Laboratory Trials	10
Director, International Programmes Branch	11
Navy Scientific Adviser	12-13
Army Scientific Adviser	14
Air Force Scientific Adviser	15
Director, Joint Intelligence Organisation	16
Director, Naval Meteorology and Oceanographic Services	17
Superintendent, RAN Research Laboratory	18
Officer-in-Charge, RAN Trials and Assessing Unit	19
Defence Information Services Branch (for microfilming)	20
Defence Library, Campbell Park	21
Library, Aeronautical Research Laboratories	22
Library, Materials Research Laboratories	23
Senior Principal Research Scientist, Laser Research Group, Materials Research Laboratories	24
District Clerk, District Council of Victor Harbor, Victor Harbor, S.A.	25
Director, Department of Marine and Harbors, Port Adelaide, S.A.	26

	Copy No.
Defence Information Service Branch for:	
Australian National Library	27
U.K., Defence Research Information Centre	28
Canada, Defence Science Information Service	29
N.Z., Ministry of Defence	30
U.S., Defense Documentation Center	31-43
WITHIN DRCS	
Chief Superintendent, Electronics Research Laboratory	44
Chief Superintendent, Weapons Systems Research Laboratory	45
Superintendent, Electronic Warfare Division	46
Superintendent, Navigation and Surveillance Division	47
Principal Officer, Night Vision Group	48
Principal Officer, Laser Group	49
Principal Officer, Optical Techniques Group	50
Principal Officer, Infra-red and Optical Countermeasures Group	51
Principal Officer, Terminal Guidance Systems Group	52
Dr D. Gambling, Infra-red and Optical Countermeasures Group	53
Mr G.W. McQuistan, Night Vision Group	54
Mr B. Russo, Optical Techniques Group	55
Author	56-57
DRCS Library	58-59
Spares	60-70